

Modeling of nutation and precession: New nutation series for nonrigid Earth and insights into the Earth's interior

P. M. Mathews

Department of Theoretical Physics, University of Madras (Guindy Campus), Chennai, India

T. A. Herring

Department of Earth, Atmospheric, and Planetary Sciences, Massachusetts Institute of Technology, Cambridge, Massachusetts, USA

B. A. Buffett

Department of Earth and Ocean Sciences, University of British Columbia, Vancouver, British Columbia, Canada

Received 28 March 2000; revised 19 December 2000; accepted 15 July 2001; published 16 April 2002.

[1] The analytical formulation of the theories of nutation and wobble reveals the combinations of basic Earth parameters that govern the nutation-wobble response of the Earth to gravitational (tidal) forcing by heavenly bodies and makes it possible to estimate several of them through a least squares fit of the theoretical expressions to the high-precision data now available. This paper presents the essentials of the theoretical framework, the procedure that we used for least squares estimation of basic Earth parameters through a fit of theory to nutation-precession data derived from an up-to-date very long baseline interferometry data set, the results of the estimation and their geophysical interpretation, and the nutation series constructed using the estimated values of the parameters. The theoretical formulation used here differs from earlier ones in the incorporation of anelasticity and ocean tide effects into the basic structure of the dynamical equations of the theory and in the inclusion of electromagnetic couplings of the mantle and the solid inner core to the fluid outer core, though this generalization comes at the cost of making some of the system parameters complex and frequency dependent; it is also more complete, as it takes account of nonlinear terms in these equations, including effects of the time-dependent deformations produced by zonal and sectorial tides, which had been traditionally neglected in nonrigid Earth theories. Among the geophysical results obtained from our fit are estimates for the dynamic ellipticity e of the Earth ($e = 0.0032845479$ with an uncertainty of 12 in the last digit), for the dynamical ellipticity e_f of the fluid core (3.8% higher than its hydrostatic equilibrium value, rather than $\sim 5\%$ as hitherto), and for the two complex electromagnetic coupling constants. Our best estimates for the RMS radial magnetic fields at the core mantle boundary and at the inner core boundary, based on the estimates for these coupling constants, are ~ 6.9 and 72 gauss, respectively, when the magnetic field configurations are restricted to certain simple classes. The field strength needed at the inner core boundary could be lower if the density of the core fluid at this boundary or the ellipticity of the solid inner core were lower than that for the Preliminary Reference Earth Model. Our estimate for the resonance frequency of the prograde free core nutation mode, with an uncertainty of $\sim 10\%$, constitutes the first firm detection of the resonance associated with this mode; the period found is ~ 1025 days, double that with electromagnetic couplings ignored. (Throughout this work, "days," referring to periods, stands for "mean solar days.") A new nutation series (MHB2000) is constructed by direct solution of the linearized dynamical equations (with our best fit values adopted for all the estimated Earth parameters) for each forcing frequency, and adding on the contributions from the nonlinear terms and other effects not included in the linearized equations. This series gives a considerably better fit to the nutation data than any of the earlier series based on geophysical theory. In particular, the residuals in the out of phase amplitudes of the retrograde 18.6 year and annual nutations, which had long remained at ~ 0.5 milliseconds of arc (mas), are now reduced to the level of the uncertainties in the observational estimates, thanks mainly to the role played by the electromagnetic couplings. The largest remaining discrepancy is that in the out of phase prograde 18.6 year nutation, of ~ 72 microseconds of arc (μas). The frequency dependence of the nutation amplitudes cannot be exactly represented through a resonance formula, nor may the resonance frequencies themselves be interpreted as the eigenfrequencies of free modes because of

the presence of complex and frequency-dependent system parameters. Nevertheless, we have constructed a new resonance formula which reproduces our nutation series accurately for almost all nutation frequencies; for the few remaining frequencies, a listing is given of the corrections to be applied in order to reproduce the exact results of the direct solution. *INDEX TERMS*: 1239

Geodesy and Gravity: Rotational variations; 1213 Geodesy and Gravity: Earth's interior—dynamics (8115, 8120); 1223 Geodesy and Gravity: Ocean/Earth/atmosphere interactions (3339); 1255 Geodesy and Gravity: Tides—ocean (4560); *KEYWORDS*: nutation series, precession rate, nutation resonance parameters, dynamical ellipticities, core electromagnetic couplings, boundary magnetic fields

1. Introduction

[2] Accurate knowledge of the variations in Earth orientation is of importance for studies in astronomy and geophysics as well as in space navigation. Space geodetic observations by techniques such as very long baseline interferometry (VLBI), lunar laser ranging (LLR), and Global Positioning System (GPS) now provide the capability to measure Earth orientation with a high precision that has improved rapidly over the past several years. Formation of a theoretical model that is accurate enough to account for the results of the measurements to within their current levels of precision would serve two purposes: to enable accurate prediction of Earth orientation and to gain information about those dynamical processes and properties of the earth, including its deep interior, that influence Earth orientation.

[3] This paper deals with one aspect of Earth orientation variations, namely, nutation. We present a new nutation series based on geophysical theory which is in much closer agreement with observational data than earlier series. The new series is based on an enhanced version of the analytical theory of *Mathews et al.* [1991a] and makes use of estimated values of seven of the parameters appearing in the theory, obtained from a least squares fit of the theory to an up-to-date nutation data set. Despite use of observational data we refer to the nutation series and amplitudes which comprise the series as “theoretical,” for convenience. In any case, as far as we are able to judge, five of our “best fit” parameters are not obtainable at present from any independent measurements with a precision anywhere near that needed for a close fit to nutation observations, and until and unless that becomes possible, any nutation series based on geophysical theory will have to rely on the use of a few parameter estimates from fits to nutation-precession data to enable the computed values to be close to observations at the level of the uncertainty in the observations. The parameters that we have estimated include the imaginary parts of two newly introduced complex parameters and certain combinations of their real parts with other basic Earth parameters. The complex parameters under reference are the Core-mantle boundary (CMB) and inner core boundary (ICB) electromagnetic coupling constants, so called because they characterize the couplings produced between the fluid outer core (FOC) and the neighboring solid regions, namely, the solid inner core (SIC) and the mantle, by the magnetic fields present at these boundaries. The estimates obtained lead to valuable new insights into deep Earth properties.

[4] Forced nutation is almost entirely due to periodic spectral components of the torques resulting from the gravitational action of celestial bodies (the Sun, the Moon, and to a minor extent, the planets) on the equatorial bulge of the Earth, though changes in matter distribution (e.g., atmospheric pressure variations) and variations in angular momentum of fluid regions relative to the solid Earth (e.g., winds) also play a small role. However, the gravitational torques are not employed directly in most approaches to the study of nutations of the nonrigid Earth. Instead, one uses a proxy, the so called rigid Earth nutation series representing the action of these torques on a hypothetical rigid Earth having the same moments of inertia and higher-order moments (as determined from observations) as the real Earth. The precision to which the amplitudes of the spectral components of rigid Earth nutation have been computed has increased by over 2 orders of magnitude in the

past few years. Compared to the accuracy of 0.01 milliseconds of arc (mas) to which the series of *Kinoshita and Souchay* [1990] has been tabulated, the recent series REN-2000 of *Souchay et al.* [1999] and RDAN of *Roosbeek and Dehant* [1998] are computed to 0.1 μ as, and the SMART series of *Bretagnon et al.* [1997, 1998] is computed to 0.01 μ as. Over the same period, the precision of estimates obtainable for the Earth orientation parameters through space geodetic methods has increased greatly. This fact, combined with the increased volume and the longer time span of the data sets now available, has made it possible to estimate from these data sets the amplitudes of a rather large number of circular nutations as well as the precession rate, with uncertainties that are almost an order of magnitude smaller than those of the early years of this decade. These developments provided the necessary wherewithal as well as the motivation to attempt significant improvements in nutation theory.

[5] The nutation series of *Wahr* [1981a, 1981c] which was adopted as the International Astronomical Union (IAU) 1980 nutation series [*Seidelmann*, 1982], has been the standard of reference ever since. This series was computed by solving the equations for the field of displacements produced by the action of the tide-generating potential (TGP) throughout the Earth, as applied to an oceanless, elastic, ellipsoidal Earth model derived under the assumption of hydrostatic equilibrium from the Earth model 1066A of *Gilbert and Dziewonski* [1975]; nutational changes in Earth orientation along with rotation rate variations and tidal deformations are encompassed in the solutions for the displacement field. The predictions of the Wahr theory have since been found to differ from observational data obtained through VLBI data analysis by much more than the uncertainties in the data. A series for practical use (referred to hereinafter as the IERS96 series) which gives close agreement to the data is now available in the International Earth Rotation Service (IERS) Conventions [*McCarthy*, 1996; see also *Herring*, 1995]. *Shirai and Fukushima* [2000a, 2000b] have constructed an improved and updated version of this series, supplemented by an estimated exponentially decaying free core nutation amplitude. Both these series are purely empirical in nature and express the nutation amplitudes in terms of a resonance formula for the transfer function in the form given by (32) and (33) of *Mathews et al.* [1991a]. The parameters in the resonance formula are determined by the basic Earth parameters (BEP) which appear in the theory, and several of the BEP are estimated through a least squares fit of the theoretical predictions to nutation amplitude estimated from the VLBI nutation time series. (The transfer function is the ratio of the function of frequency describing the amplitudes of circular nutations of the “real” Earth to the corresponding function for the rigid Earth.) Physical considerations show that the parameters in this resonance formula must obey two sum rules [see, e.g., *Mathews and Dehant*, 1995]. The sum rules were not used in the construction of the IERS series because at that time, the degradation of the fit resulting from the enforcement of the sum rules was of an extent that detracted from the primary aim of generating a series which matched the data well; they are not enforced in the Shirai-Fukushima series either. The values obtained for the resonance parameters from these fits do not therefore admit interpretation in geophysical terms.

[6] A major step toward a better geophysical accounting of nutation was already taken by *Gwinn et al.* [1986] and *Herring et al.* [1986], with their finding that a value $\sim 5\%$ higher than that of

the hydrostatic equilibrium state is needed for the dynamical ellipticity of the fluid core to close the gap of ~ 2 mas found between the observed and the IAU 1980 values for the in phase part of the amplitude of the retrograde annual nutation. Modeling and numerical computations of the effects of ocean tides [Sasao and Wahr, 1981; Wahr and Sasao, 1981] and of mantle anelasticity [Wahr and Bergen, 1986] were other important contributions to nutation theory. Detailed Earth models with nonhydrostatic equilibrium structure have been constructed recently, and their nutations were computed [Dehant and Defraigne, 1997; Schastok, 1997] using an approach similar to that of Wahr [1981a, 1981c]. In the model of Defraigne [1997], employed in the first of these works, mantle convection was invoked for generating the extra (nonhydrostatic) ellipticity, while the dynamical mechanism responsible is not spelled out in Schastok's work which incorporates ocean tide excitation too into the model. A systematic presentation of the formalism and comparisons of numerical results with those of others are given by Huang *et al.* [2001], whose approach is similar to Schastok's.

[7] A different approach based on the torque equations for the ellipsoidally stratified deformable Earth and its core regions, pioneered by Molodensky [1961], reformulated elegantly by Sasao *et al.* [1980], and generalized by Mathews *et al.* [1991a] to include the dynamics of the inner core, encapsulates those properties of the Earth that are relevant to nutations in a set of ellipticity, compliance, and other parameters. The torque equations and an accompanying kinematical equation reduce, in the frequency domain, to a set of simultaneous linear algebraic equations in which the role of the abovementioned parameters is entirely transparent. The insight provided by such parameterization was crucial for the inference of nonhydrostatic ellipticity, referred to above, and in the use (by Buffett [1992]) of an electromagnetic coupling at the core mantle boundary to account for the residual of ~ 0.4 mas that remained in the out of phase part of the retrograde annual amplitude after taking account of anelasticity (AE) and ocean tide (OT) effects.

[8] Yet another approach, developed and pursued by J. Getino, J. M. Ferrandiz, and collaborators in numerous papers over the past several years [see Getino and Ferrandiz, 1999, 2000a, 2000b, and references therein], is based on the canonical formalism of Kinoshita [1977] with modifications to take account of the nonrigidity of the Earth and the presence of its core regions. The last of these papers claims a better fit to the IERS96 nutation series (not to the observationally estimated series) than all other existing theories and states that the computed values are for a nonrigid Earth comprising a mantle, FOC, and SIC, with a delay in the elastic response allowed for and with oceanic corrections added on; no particulars are given of the theory or of any parameter fit done for optimizing the agreement with the IERS96 series. No publication giving the essential details of the work leading to the stated result (the theoretical framework and the Earth model employed, the identity and physical meaning of the parameters adjusted in the fitting process, and the estimates obtained from the fit for these parameters and their physical interpretation) has appeared yet, to our knowledge, nor has any preprint been available to us. Therefore we base our discussion of the approach of these authors on the work of Getino and Ferrandiz [1999], which provides some details, although like Getino and Ferrandiz [2000a], it employs a two-layer Earth model lacking in some essential features: the mantle is treated as rigid in the latter, while ocean tide effects (which are up to 2 orders of magnitude larger than current uncertainties in the amplitudes estimated from nutation data) are left out altogether in the former work in fitting the theory to the IERS96 series. A major problem with the fits stems from the parameters chosen for adjustment. Three of the critical parameters, which are independently adjusted, are the scale parameters k_M and k_S of Kinoshita [1977] representing the respective abilities of the Moon and the Sun to exert torques on the Earth and the ratio (A_c/A_m) of the moments of inertia of the core and the mantle. Apart from rescaling the relative

magnitude of the lunar and solar terms in the nutation series, the adjustment of k_M and k_S leads to estimated values that are incompatible with the precisely known values of the astronomical parameters in terms of which they are defined, as will be shown later. For a recent review of observational and theoretical aspects of nutations, see Dehant *et al.* [1999].

[9] In the present work, the dynamical equations of Mathews *et al.* [1991a] are modified by including in their basic structure (1) the effects of mantle anelasticity, (2) the effects of ocean tides, (3) the electromagnetic couplings produced between the FOC, on the one hand, and the mantle and the SIC, on the other hand, at the frequencies of the wobbles, because of magnetic fields crossing the CMB and the ICB, and (4) nonlinear terms which have hitherto been ignored in this type of formulation. After an overview, at the beginning of the section 2, of the salient features of the unmodified theory including the representation of nutation amplitudes in terms of resonance formulae in different forms, the modeling of the abovementioned effects is explained, including, in particular, the procedure adopted for construction of empirical ocean loading and current admittance functions needed for this purpose. The manner in which the various effects are integrated into the theory is elucidated, and the important fact that several of the system parameters become complex and frequency dependent in this process is pointed out. The nature of the dependence of nutation amplitudes on the basic parameters of the theory is discussed next, and those parameters that are most appropriate for estimation through a least squares fit to data are identified. Treatment of the nonlinear terms in the dynamical equation and their contributions is left to Appendix A. The dominant nonlinear terms represent the effects of the nearly diurnal tidal potential on the time-dependent deformations due to the zonal potential, first considered by Souchay and Folgueira [2000], and on those due to the sectorial potential, not considered before.

[10] We introduce in section 3 the nutation-precession data set used in our study. Details regarding the VLBI data set from which these are derived and the data analysis procedures used may be found in the accompanying paper by Herring *et al.* [2002]. The procedure employed for our least squares fit is briefly outlined next, following a discussion of steps to take account of effects not included in the theoretical expressions that are used for the fitting. Presentation of the values found for the various basic Earth parameters estimated through the fit and discussion and interpretation of the estimates are done in section 4. The reader whose primary interest is in the geophysical aspect of our results may want to proceed directly to section 4 and return to earlier sections as needed.

[11] Given the values of the basic Earth parameters, one can use the method explained in Appendix B to compute the corresponding values for the parameters in a reduced resonance formula of the form given in section 2. The numerical values obtained thus for the resonance parameters are presented and discussed in section 5. The seemingly unrealistic values obtained for both the real and the imaginary parts of the Chandler resonance frequency are shown to be a consequence of the complex and frequency dependent value of the relevant compliance parameter of the anelastic Earth with oceans. The considerations involved are discussed on the basis of general physical principles in Appendices C and D, which are essential reading to avoid being led by the unfamiliar aspects of some of our results into misinterpreting them in physical terms. In section 6, we explain the construction of our new nutation series MHB2000 by direct solution of the linearized dynamical equations with the use of values obtained from the least squares fit for those Earth parameters that are estimated; the series includes corrections for effects not included in these equations. We proceed then to present a new resonance formula, (42), which reproduces this series exactly except for a few frequencies; for these frequencies the corrections to be applied to the resonance formula results are listed. We conclude with remarks in section 7 on a few points to supplement the discussion in the earlier sections.

[12] The highlights of the geophysical results reported in the present work, which go hand in hand with the new nutation series, are the following: Strong evidence has been found for the first time for the prograde free core nutation mode which had been theoretically predicted by *Mathews et al.* [1991a, 1991b] and *de Vries and Wahr* [1991] as a consequence of the role of the SIC in nutation dynamics. The evidence comes from the associated resonance in the forced nutations, with a period of ~ 1025 days, double what was predicted by the above authors; the difference is understood in terms of the effects of the magnetic field at the ICB. For the Chandler resonance we find a period of ~ 383 days; while this value is surprising at first sight, we have shown that it does lead to a period of 430 days for the free Chandler wobble, in agreement with observations, when one takes quantitative account of the difference between the values of the anelastic and ocean tide response parameters at widely differing frequencies: the nearly diurnal tidal frequencies responsible for nutations, on the one hand, and the low frequency of the free Chandler wobble, on the other hand. An estimate of 3.2845479×10^{-3} with an uncertainty of under 0.4 parts per million has been obtained for the dynamical ellipticity $e \equiv (C - A)/A$ of the Earth, where C and A are the polar and mean equatorial principal moments of inertia of the Earth respectively. The corresponding value of $H_d \equiv (C - A)/C$ is 3.2737949×10^{-3} . The smallness of the uncertainty is attributable to the use, in the estimation process, of a large number of quantities sensitive to the value of e : the amplitudes of all the nutations used for our analysis, as well as the precession rate. We have also obtained estimates for the RMS values of the radial component of the magnetic fields at the CMB and the ICB (~ 6.9 and 72 gauss, respectively) and for the dynamic ellipticity of the fluid core (3.8% in excess over the hydrostatic equilibrium value). These have been inferred from the estimates obtained for the imaginary parts of the CMB and ICB electromagnetic coupling constants and for their real parts in combination with certain other Earth parameters. A general relation connecting the real and imaginary parts of the electromagnetic coupling constants has been made use of in this process, with evaluation of the relation done only for certain restricted classes of configurations of the magnetic field. Also employed was information from Magsat data about the dipole component of the CMB magnetic field. The existence of a mantle bottom layer of conductivity equal to that of the core fluid and of thickness ~ 210 m was assumed; if the thickness or the conductivity were lower, the CMB field strength called for by the observed coupling would be higher. In respect of the ICB, the ellipticity of the SIC and the density of the core fluid as well as the density contrast at the ICB were taken to be the same as for a hydrostatic equilibrium Earth. A discussion of the extent to which estimates for the magnetic field strength (especially at the ICB) could be modified by changes in the assumed values may be found in section 7.

[13] Figures referred to herein as the “uncertainties” in the quantities estimated on the basis of our least squares fit are the respective formal standard deviations scaled up by 2.8. The reason for the scaling is that the realistic uncertainties in our input data are larger than their formal sigmas (see section 3.1 and *Herring et al.* [2002]). The scale factor has been chosen as the square root of the chi squared per degree of freedom obtained for the fit between theory and data.

2. Theoretical Considerations and Outline of Formalism

[14] The analytic formulation given by *Mathews et al.* [1991a] for the theory of wobbles and nutations of an oceanless, elastic, axially symmetric ellipsoidal Earth with a mantle, FOC, and SIC (hereinafter referred to as the “basic Earth”) was a development of

the torque equations for the Earth and its core regions together with a kinematic equation relating the variations in orientation of the SIC to its angular velocity variations. These equations are intrinsically nonlinear, but a linear approximation was traditionally employed in the past, as the effect of the nonlinear terms was deemed to be too small to merit attention.

[15] However, preliminary studies by one of us (P.M.M.) together with Pierre Bretagnon indicated that the neglected terms could have nonnegligible effects on nutations, and the recent work of *Souchay and Folgueira* [2000] on the effect of zonal deformations on the nutations of an otherwise rigid Earth has shown that this is indeed the case. The effects of deviations from the linearized theory are dealt with in Appendix A, where an expression is derived for the resulting contribution to nutation amplitudes.

[16] The torque equations determine the wobbles (and spin rate variations), which may be viewed as the terrestrial manifestation of nutation and axial rotation variation in space. These celestial motions are related to the terrestrial ones through kinematic equations which are independent of the structure and properties of the Earth. The kinematic relations in their full nonlinear form are given by *Bretagnon et al.* [1997]. The only appreciable effect resulting from the nonlinearities in these relations is on the obliquity, through the role of spin rate variations (or, equivalently, UT1 variations); it is rather large, having an amplitude of ~ 0.7 mas with an 18.6 year period, as shown by *Bretagnon et al.* [2000]. However, on account of the way in which UT1 variations are incorporated into the transformation matrix relating terrestrial and celestial reference frames in the algorithm for VLBI data analysis [see, e.g., *McCarthy*, 1996], this effect does not show up in the nutation series resulting from the analysis. For this reason, it is quite sufficient to use the linearized version of the kinematic relation, and we shall do so.

[17] The linearized approximation to our formulation for the torque equations including AE and OT effects and electromagnetic couplings is outlined in sections 2.1–2.5. Electromagnetic torques at the nearly diurnal frequencies of the wobbles arise because Lorentz forces are brought into play by magnetic fields crossing the boundaries of the FOC when differential rotations between the FOC and the other regions take place as a concomitant of nutation. The electromagnetic coupling parameters are complex, and anelasticity is represented through complex increments to deformability parameters of the different regions of the Earth. Both these sets of parameters vary only very slightly over the diurnal frequency band. If this variation is ignored, the structures of the theoretical expressions that appear in our treatment, such as resonance formulae and approximate expressions for resonance frequencies and coefficients, will remain unaffected by these effects, although a number of real parameters get replaced by complex ones. The inclusion of ocean tide effects, also done through complex increments to deformability parameters, is more problematic, for the simple reason that the OT admittance has a large variation with frequency within the diurnal band. (By “admittance” we mean the amplitude of the spherical harmonic degree 2 and order 1 part of the ocean tide per unit amplitude of the TGP component that excites the tide.) The variation is caused both by the strong frequency dependence associated with the free core nutation (FCN) resonance in the diurnal ocean tides and by ocean dynamic factors unconnected with the FCN, like ocean geometry and bathymetry. We use an empirical formula, deduced as explained in section 2.5, to represent the frequency dependence of the admittance. Resonance formulae for the transfer function and limitations on it are discussed in this context. Section 2.6 deals with the accounting of contributions to nutations from sources unrelated to the TGP. Developments in the nutation theory for the rigid Earth are considered in section 2.7. We then go on to a discussion, in section 2.8, of the parameters that may be expected to have a significant influence on nutations. Our ana-

lytical formalism makes possible the identification of such parameters, which is a prerequisite to the fitting of a dynamical theory to observational data.

2.1. Analytical Formulation for the Basic Earth: Linear Approximation

[18] Consider a forced or free nutation having an angular frequency of τ cycles per sidereal day (cpsd) in space, 1 cpsd being the frequency of the mean diurnal rotation of the Earth with an angular velocity $\Omega_0 = 7.292115 \times 10^{-5} \text{ rad s}^{-1}$. The nutation is accompanied by a wobble of the Earth's mantle, i.e., a circular motion of its rotation axis around its geometric axis, with frequency σ cpsd as seen from the rotating Earth, where

$$\sigma = \tau - 1. \quad (1)$$

(The term “geometric axis” or “symmetry axis” will be used herein to refer to the direction of the principal axis of maximum moment of inertia, with tidal deformations ignored, in an axially symmetric approximation for the Earth.) The amplitude $\tilde{m}(\sigma)$ of this wobble, the amplitudes $\tilde{m}_f(\sigma)$ and $\tilde{m}_s(\sigma)$ of accompanying wobbles relative to the mantle of the FOC and SIC, and the amplitude $\tilde{n}_s(\sigma)$ of the offset of the polar axis of the SIC from that of the mantle are the dynamical variables of the wobble-nutation problem in the frequency domain.

[19] It was shown by Mathews *et al.* [1991a] in the linearized approximation that the four-component column $x(\sigma)$ having these dynamical variables as elements obeys a matrix equation

$$M(\sigma)x(\sigma) = \tilde{\phi}(\sigma)y(\sigma), \quad (2)$$

where $\tilde{\phi}(\sigma)$ is the amplitude in nondimensional form of the relevant spectral component of the TGP. Equation (2) contains in succinct form the equatorial components of the equations of angular momentum balance for the whole Earth, the FOC, and the SIC together with the kinematic equation which relates the instantaneous orientation of the symmetry axis of the SIC to that of its rotation axis. Equation (2) will be referred to in the following as the linearized dynamical equation (LDE) of the wobble-nutation problem since small terms that are nonlinear in the dynamical variables were neglected in writing it down.

[20] As may be seen from (26) of Mathews *et al.* [1991a], the dynamical matrix M and the column vector y have the forms

$$M = F + \sigma G, \quad y = y_c + \sigma y_t, \quad (3)$$

where the elements of the 4×4 matrices F and G and of the columns y_c and y_t are simple combinations of certain basic Earth parameters (BEP). In the theory of Mathews *et al.* [1991a] for the basic Earth, the BEP, which were all real, consisted of the dynamical ellipticities, e , e_f , and e_s and the mean equatorial moments of inertia A , A_f and A_s of the Earth, the FOC, and the SIC, the compliance parameters κ , γ , ξ , β , \dots , representing the deformabilities of the Earth and of its core regions under different types of forcing, the density ρ_f of the outer core fluid at the inner core boundary (ICB), and certain other parameters (α_g , A' , and e') needed for characterization of the gravitational coupling between the SIC and the rest of the Earth. Axial symmetry of the Earth has been invariably assumed in the literature of nutations of the nonrigid Earth. Against this background, A will be taken in this paper to stand for the mean of the two principal equatorial moments of inertia, $(A + B)/2$; similar meanings are taken for A_f and A_s . With this understanding the Earth's dynamical ellipticity or dynamical flattening is $e = (C - A)/A$, with similar notation for e_f and e_s of the core regions. Triaxiality, i.e., inequality of A and B , gives rise to semidiurnal nutations, which will be considered in a separate publication. Diurnal nutations due to higher moments of the Earth's structure will also be considered separately.

[21] The reader is referred to Mathews *et al.* [1991a] for precise definitions of the various parameters, derivations, and other details. It may be noted that the Love number k with the deformational effects of wobbles excluded is directly related to the compliance κ [see Mathews *et al.*, 1995]:

$$\kappa = \frac{\Omega_0^2 a^5}{3GA} k^{(nw)},$$

where the superscript *nw* means “no wobbles.” It represents the deformability of the whole Earth (and γ , that of the fluid core region alone) under degree 2 tidal forcing, while β characterizes the deformability of the FOC under the centrifugal forcing associated with the wobble of the FOC relative to the mantle.

[22] Given the values of the BEP, solution of (2) yields the amplitudes $\tilde{m}_f(\sigma)$, $\tilde{m}_s(\sigma)$, and $\tilde{n}_s(\sigma)$ produced by the given spectral component of the TGP. In particular,

$$\tilde{m}(\sigma) = [M^{-1}(\sigma)y(\sigma)]_1 \tilde{\phi}(\sigma), \quad (4)$$

wherein the quantity in brackets is a four-component column vector, and the subscript 1 indicates the first element of this vector.

[23] The dynamical ellipticity e is the only parameter relevant to the free (Eulerian) and forced wobbles of a hypothetical rigid Earth (ellipsoidal, with axial symmetry). The wobble amplitude $\tilde{m}_R(\sigma)$ (subscript *R* for “rigid”) has the simple expression

$$\tilde{m}_R(\sigma) = \frac{e}{e - \sigma} \tilde{\phi}(\sigma). \quad (5)$$

This result follows trivially from the explicit form of (2) when the compliances are set equal to zero in M and y .

[24] The amplitude $\tilde{\eta}(\sigma)$ of the nutation associated with the wobble of frequency σ cpsd is related to $\tilde{m}(\sigma)$ by

$$\tilde{\eta}(\sigma) = -\frac{\tilde{m}(\sigma)}{1 + \sigma}. \quad (6)$$

This is the linearized approximation [Ooe and Sasao, 1974] to the kinematic relation referred to earlier, which holds irrespective of the Earth's structure and elastic properties. It follows then that the transfer function $T(\sigma; e)$ from the amplitude for the rigid Earth to that of the nonrigid Earth is the same for the wobble and the corresponding nutation:

$$T(\sigma; e) \equiv \frac{\tilde{\eta}(\sigma)}{\tilde{\eta}_R(\sigma)} = \frac{\tilde{m}(\sigma)}{\tilde{m}_R(\sigma)} = \frac{e - \sigma}{e} [M^{-1}(\sigma)y(\sigma)]_1. \quad (7)$$

[25] The transfer function $T(\sigma; e)$ has a resonance expansion [Mathews *et al.*, 1991a] of the form,

$$T(\sigma; e) = R + R'(1 + \sigma) + \sum_{\alpha} \frac{R_{\alpha}}{\sigma - \sigma_{\alpha}}. \quad (8)$$

The resonance frequencies σ_{α} are associated with four free nutation/wobble modes: the Chandler wobble (CW), two free core nutations (FCN or RFCN, which is the retrograde nutation induced by the ellipticity of the fluid core, and PFCN, a prograde nutation which owes its existence to the presence of an elliptical solid inner core) and a free wobble of the inner core (ICW). The σ_{α} are obtained by solving the homogenous equation $Mx = 0$, or equivalently, the eigenvalue equation $Lx = \sigma x$, where $L = F^{-1}G$. The existence of the resonance expansion, (8), follows solely from the linear dependence of the M_{ij} and the y_i on σ , mentioned earlier, and that of $1/\tilde{m}_R(\sigma)$, evident from (5). The nature of the

dependence of these quantities on the BEP is not relevant for this purpose.

[26] The explicit forms of M and y [see Mathews *et al.*, 1991a] imply also that at $\sigma = -1$ (corresponding to zero frequency, $\tau = 0$, in inertial space) the wobble amplitude of the nonrigid Earth is just the same as for a rigid Earth having the same ellipticity e :

$$\tilde{m}(-1) = \tilde{m}_R(-1), \quad \text{implying } T(-1; e) = 1. \quad (9)$$

(This is the property that *Poincaré* [1910] designated as “gyrostatic rigidity.”) We also note that by virtue of the definition (7) of $T(\sigma; e)$ and the form (5) of $\tilde{m}_R(\sigma)$,

$$T(\sigma; e) = 0 \quad \text{at} \quad \sigma = e. \quad (10)$$

Equations (9) and (10) lead to two sum rules for the set of parameters appearing in (8):

$$\begin{aligned} R &= 1 + \sum_{\alpha} \frac{R_{\alpha}}{1 + \sigma_{\alpha}} \\ R'(1 + e) &= -R - \sum_{\alpha} \frac{R_{\alpha}}{e - \sigma_{\alpha}}. \end{aligned} \quad (11)$$

These may be used to express R and R' in terms of the resonance frequencies σ_{α} and coefficients R_{α} . The result is a new form for the resonance formula:

$$T(\sigma; e) = \frac{e - \sigma}{e + 1} \left(1 + (1 + \sigma) \sum_{\alpha=1}^4 \frac{N_{\alpha}}{\sigma - \sigma_{\alpha}} \right). \quad (12)$$

[27] When the ellipticity e is one of the parameters to be estimated by fitting theoretical expressions to VLBI estimates of both the precession rate and the amplitudes of a set of circular nutations, one has to allow for a possible difference between the eventual estimate for e and the value e_R assumed in the construction of the rigid Earth series. In such a situation it is necessary to consider a generalized transfer function $T(\sigma; e|e_R)$ from the amplitude $\tilde{\eta}_R(\sigma; e_R)$ for a rigid Earth of ellipticity e_R to the amplitude $\tilde{\eta}(\sigma; e)$ of a nonrigid Earth with a different ellipticity e . Explicitly,

$$\begin{aligned} \tilde{\eta}(\sigma; e) &= T(\sigma; e|e_R) \tilde{\eta}_R(\sigma; e_R) \\ T(\sigma; e|e_R) &= (1 - \sigma/e_R) [M^{-1}(\sigma)y(\sigma)]_1. \end{aligned} \quad (13)$$

The last expression is obtained by dividing (4) by (5), with e replaced by e_R in the latter.

[28] The transfer function (13) may be expressed as an explicit analytic function of σ and the BEP by inversion of the 4×4 matrix $M(\sigma)$, and the function can be separated into terms of different orders in the BEP. However, terms beyond the first order are too complicated to be really enlightening, and direct numerical evaluation of $M^{-1}(\sigma)$ is far simpler than evaluation of such an analytical expression.

[29] It is easy to show that the generalized transfer function may be expressed in the form

$$\begin{aligned} T(\sigma; e|e_R) &= \frac{e_R - \sigma}{e_R + 1} \\ &\cdot N_0 \left(1 + (1 + \sigma) \sum_{\alpha=1}^4 \frac{N_{\alpha}}{\sigma - \sigma_{\alpha}} \right). \end{aligned} \quad (14)$$

The term “reduced resonance formula” (RRF) will hereinafter refer to (14), while (8) with parameters not constrained to obey the

sum rules (11) will be referred to as the unconstrained resonance formula (URF). The value of N_0 and the relations between the resonance coefficients in (8) and (14) are as follows:

$$\begin{aligned} N_0 &= \frac{H_d}{H_{dR}} = \frac{e/(1 + e)}{e_R/(1 + e_R)} \\ R_{\alpha} &= \frac{(e_R - \sigma_{\alpha})}{(1 + e_R)} (1 + \sigma_{\alpha}) N_0 N_{\alpha}, \end{aligned} \quad (15)$$

where $H_d \equiv e/(1 + e)$ is what is referred to in the literature of astronomy as the dynamical ellipticity of the Earth. For the generalized transfer function, the sum rules (11) get replaced by

$$\begin{aligned} R &= N_0 + \sum_{\alpha} \frac{R_{\alpha}}{1 + \sigma_{\alpha}} \\ R'(1 + e_R) &= -R - \sum_{\alpha} \frac{R_{\alpha}}{e - \sigma_{\alpha}}. \end{aligned} \quad (16)$$

2.2. Inclusion of Various Effects: General Remarks

[30] We show in sections (2.3)–(2.5) how the formalism just presented, which assumes the BEP to be frequency independent, may be generalized to incorporate anelasticity and ocean tide effects and electromagnetic couplings. The last of these introduces complex coupling parameters into the dynamical matrix, and complex increments to the compliances arise from the other two effects. Furthermore, the increments due to the ocean tides depend strongly on the excitation frequency σ . While complexification does not affect the above formalism except to make the σ_{α} and N_{α} complex, frequency dependence of parameters in F and G (and hence in L) has the important consequence that an eigenvalue σ_{α} of L will not, in general, be the frequency of a free wobble mode. The reason for this seemingly radical departure from the familiar picture is simple enough. In a wobble normal mode the centrifugal perturbation due to the wobble and the deformation caused by it have the same frequency as the wobble itself; therefore the compliances, which characterize the extent and phase of the deformations, must necessarily appear with values pertaining to the frequency of the free mode in the homogeneous equation to be solved for determining that frequency, namely, (2), with ϕ set equal to zero, or equivalently, $Lu^{\alpha} = \sigma_{\alpha}u^{\alpha}$ (see Appendix B). Stated differently, a particular eigenvalue of L , say σ_1 , can be the physical eigenfrequency of a free wobble only if L is constructed with values appropriate to the frequency σ_1 itself in the first place, and when this is done, the other σ_{α} , $\alpha \neq 1$, are not the frequencies of any free wobble modes. From the mathematical point of view, these strange features are a consequence of the fact that $Lu^{\alpha} = \sigma_{\alpha}u^{\alpha}$ is not a linear eigenvalue problem when the matrix L itself is frequency dependent. If L is evaluated at some forcing frequency σ_0 in the retrograde diurnal band, its eigenvalue σ_1 having real part near $1/400$ cannot be the frequency of the free Chandler mode because the values used for the compliances present in L do not pertain to this frequency. There can be no free mode associated with this σ_1 ; otherwise, there would be a host of “free Chandler wobbles,” one associated with each of the distinct values of σ_1 that would result from different choices of σ_0 . One can proceed, of course, as in Appendix B, to construct a resonance formula in terms of the eigenvalues σ_{α} and eigenvectors u_{α} and \tilde{v}_{α} pertaining to L evaluated at some forcing frequency σ_0 in the retrograde diurnal band, ignoring thereafter the fact that these quantities vary with the σ_0 . The σ_{α} clearly play the role of resonance frequencies in (8), though the formula cannot be exact for any forcing frequency other than σ_0 . The exact solution is given by (13), and it is by numerically evaluating this solution for every frequency of interest and fitting the results to the data after taking account of terms and effects not incorporated into the LDE that we

gain the most information relevant to the geophysical interpretation of nutations. Nevertheless, the approximate analytical expressions available for the eigenvalues play a vital role in the least squares fitting process, as we shall see.

[31] One might wonder why it is worthwhile to invite such complications by incorporating all the effects into the dynamical equations. The answer lies in the fact that the results obtained on including all the effects together differ from the sum of the contributions, separately evaluated, from the individual effects. We find, for instance, that the individual contributions from anelasticity, ocean tidal loading, currents, and CMB and ICB couplings to the out of phase retrograde 18.6 year nutation are $-0.155, 0.986, -0.020, 0.249$, and 0.278 mas, respectively, adding up to 1.339 mas in all, while the combined effect is 1.358 mas. As another example, the corresponding numbers for the in-phase retrograde annual nutation are $0.267, 0.174, 0.000, -0.450$, and -0.012 , for a total of -0.021 mas, compared to the combined effect of -0.048 mas; for the out of phase part the sum of the individual contributions is 0.304 mas, while the combined effect is 0.331 mas. The need for an integrated approach when dealing with high-precision data is thus evident.

[32] In computing the frequencies σ_α and strength parameters N_α presented in section 5, the ocean tide contributions to the compliance parameters in M have been assigned values pertaining to the forcing frequency σ_{R18} (-1.0001467 cpsd), very close to the median frequency of the diurnal tidal band, which corresponds to the retrograde 18.6 year (R18) nutation. The ocean tide contributions to nutation amplitudes are, according to the theoretical estimates, of the order of one part in a thousand or less, and the nonconstancy of the ocean tide admittance is responsible only for a part of these contributions. There is also a very minor but not entirely negligible variation across the diurnal band due to the ω dependence of the electromagnetic coupling, seen from (19), and that of the anelasticity factor F of (17b). These have been taken into account in our final fits and in the evaluation of the exact solutions.

2.3. Inclusion of Anelasticity Effects

[33] Mantle anelasticity causes a small frequency-dependent phase lag in the Earth's response to periodic forcing besides altering the magnitude of the response. Stated differently, anelasticity causes the shear and bulk moduli (at any point within the mantle) to become complex and frequency dependent. In the anelasticity models with no bulk dissipation proposed by *Sailor and Dziewonski* [1978] and *Sipkin and Jordan* [1980] and in variants of them treated in detail by *Wahr and Bergen* [1986], the variation of the shear modulus with the excitation frequency ω is represented by

$$R(\omega, r) \equiv \frac{\delta\mu(\omega, r)}{\mu_0(r)} = \frac{F(\omega; \omega_m, \alpha)}{Q_\mu(\omega_m, r)} \quad (17a)$$

$$F(\omega; \omega_m, \alpha) = \cot\left(\frac{\alpha\pi}{2}\right) \left\{ 1 - \left(\frac{\omega_m}{\omega}\right)^\alpha \right\} - i s_\omega \left(\frac{\omega_m}{\omega}\right)^\alpha, \quad (17b)$$

where $\mu_0(r)$ is the real part of the shear modulus of the anelastic Earth at the radial position r at the reference frequency ω_m in the seismic frequency range, α is the index of the assumed power law variation of the quality factor Q_μ of mantle dissipation, and $\delta\mu(\omega, r) = \mu(\omega, r) - \mu_0(r)$. The appearance of $s_\omega \equiv (\omega/|\omega|)$ has to do with the choice of sign convention for tidal frequencies (see Appendix C). Clearly, $\delta\mu$ depends on the values chosen for the parameters ω_m and α , although we have not explicitly indicated this in the notation. It is assumed by *Sailor and Dziewonski*, *Sipkin and Jordan*, and *Wahr and Bergen*, that Q_μ has constant values within the upper mantle and within the lower mantle. Other models of mantle Q which allow for variation within each of these regions are available [e.g., *Widmer et al.*, 1991]. The function $\mu_0(r)$ is

determined from seismic data, and ω_m is an average frequency which is representative of the range of frequencies to which the seismic data used pertain. Note that the imaginary part of the shear modulus $\mu(\omega_m, r)$ at the reference frequency is included in $\delta\mu$ as given by the above formula: $\text{Im } \delta\mu(\omega_m, r) = -s_\omega \mu_0 / Q_\mu(\omega_m, r)$.

[34] The compliances appearing in nutation theory are computed initially for an elastic Earth model, such as Preliminary Reference Earth Model (PREM) of *Dziewonski and Anderson* [1981], by integrating the equations of tidal deformation (see, for instance, *Buffett et al.* [1993], who consider also the small contributions to the compliances from the Earth's ellipticity and from the Coriolis force due to Earth rotation as well as from differential rotations of the FOC and SIC relative to the mantle). The anelasticity contributions to the compliances at the median frequency ω_d of the diurnal band (i.e., the 1 cpsd frequency of the K_1 tide) are computed from the same deformation equations by evaluation of the changes in deformations resulting from replacement of $\mu_0(r)$ by $\mu_0(r) + \text{Re } \delta\mu(\omega_d, r)$ and, again, by $\mu_0(r) + \text{Im } \delta\mu(\omega_d, r)$ and then taking the complex combination of the two. ($\delta\mu(\omega_d, r)$ is obtained, of course, by introducing (17b) in (17a).) The default option that we use for the anelasticity model has $\alpha = 0.15$ and a reference period of 200 s ($\omega_m = 2\pi/200$), with rheology as given by *Dziewonski and Anderson* [1981]. The effect of switching to other values for these parameters or even to other anelasticity models is just to change the real and imaginary parts of F by appropriate factors f_r and f_i . These changes simply cause the real parts of the anelasticity contributions to all the compliances to be multiplied by the common factor f_r and the imaginary parts to be multiplied by the common factor f_i . The two compliances to which the nutations are most sensitive, namely, κ and γ , are estimated during our least squares fitting procedure (see section 2.8); therefore any change in f_r would merely alias into changes in the estimates obtained for these parameters and would not lead to an improvement in the quality of the fit. We have explored how the fit is affected on changing f_i from unity. We found that the fit improves initially with increasing f_i but degrades rapidly beyond a point. The optimum value was $f_i = 1.09$. We have incorporated this scaling into what we call the default model hereafter.

2.4. Inclusion of Electromagnetic Couplings

[35] *Buffett* [1992] computed the contribution to nutations from the diurnally varying torque produced between the differentially wobbling FOC and mantle by the magnetic field present at the CMB. This torque is proportional to m_f , and that between the FOC and the SIC, caused by the magnetic field at the ICB, is proportional to $(m_f - m_s)$. Therefore their presence modifies the coefficients of \tilde{m}_f and \tilde{m}_s in the angular momentum balance equations for the FOC and the SIC and hence the corresponding elements of the dynamical matrix M . There are four such elements. The expressions given in (26b) of *Mathews et al.* [1991a] for these elements are now to be modified as follows:

$$M_{22} \rightarrow M_{22} + K^{\text{CMB}} + K^{\text{ICB}} A_s / A_f, \quad (18a)$$

$$M_{23} \rightarrow M_{23} - K^{\text{ICB}} A_s / A_f, \quad (18b)$$

$$M_{32} \rightarrow M_{32} - K^{\text{ICB}}, \quad (18c)$$

$$M_{33} \rightarrow M_{33} + K^{\text{ICB}}, \quad (18d)$$

wherein K^{CMB} and K^{ICB} are complex coupling strength parameters representing the influence of the respective torques. They are to be counted henceforth among the BEP.

[36] K^{CMB} in the \tilde{m}_f term (M_{22}) of the equation for the FOC and K^{ICB} in the \tilde{m}_s term (M_{33}) of the equation for the SIC have parallel roles and should be expected to have the same sign for

their real parts. This sign is positive, as has been found for $\text{Re } K^{\text{CMB}}$ in the work by Buffett [1992]. This is indeed what one expects on physical grounds: e_f in M_{22} , which represents the inertial coupling between the core and the mantle due to the ellipticity of the CMB, appears with a positive sign, and $\text{Re } K^{\text{CMB}}$ should have the same sign since the presence of a magnetic field is expected to strengthen the coupling. As for the imaginary parts of the K parameters, their signs should be such as to represent dissipation and should therefore be the same as the signs of imaginary parts arising from the compliances already present in M_{22} and M_{33} .

[37] The theory which enables one to interpret the estimates obtained for the electromagnetic coupling parameters in geophysical terms is presented by Buffett *et al.* [2002], who discuss the assumptions and approximations made; that paper may be consulted for all details. The salient points are reproduced here for convenience. The conducting material of the mantle, FOC, and SIC undergoes motion relative to the main magnetic field $\mathbf{B}(\mathbf{r})$ in the course of the differential wobbles of these regions. The current which gets generated then by electromagnetic induction and the induced magnetic field $\mathbf{b}(\mathbf{r})$ due to this current distribution oscillate with the nearly diurnal frequency of the wobble motion. The Lorentz force exerted on the current-carrying elements of matter perturbs the fluid flow near the CMB and the ICB, and this perturbation, in turn, affects the current induced. Therefore the induction equation and the equation governing the perturbation of the fluid flow (in which the Coriolis force plays a nontrivial role) constitute a coupled system. Solution of this system, subject to the usual continuity conditions on the magnetic field and boundary conditions relating the fluid velocity to the differential wobbles, leads to expressions for the induced fields $\mathbf{b}(\mathbf{r})$ at the CMB and ICB and hence for the integrated torques on the FOC and SIC at the wobble frequency due to the Lorentz force. If the radial component of the main field $\mathbf{B}(\mathbf{r})$ is denoted by B_r , and the complex combination $(\Gamma_1 + i\Gamma_2)$ of the equatorial components of the electromagnetic torque is denoted by $\tilde{\Gamma}$, one obtains,

$$\tilde{\Gamma}^{(b)}(\sigma) = \frac{-ia_b^2 \Omega_0}{8\mu_0} \left(\frac{1}{2\bar{\eta}_b |\omega|} \right)^{1/2} (\Delta \tilde{m})_b I_b, \quad (19)$$

where μ_0 is the magnetic permeability of the vacuum and $\omega = \Omega_0 \sigma$. Here b refers to the boundary in question ($b = c$ for the CMB and s for the ICB), a_b is the radius of the boundary, assumed to be spherical ($a_b = a_c$ for the CMB and a_s for the ICB), and I_b is the integral of B_r^2 , weighted by a certain factor, over the boundary. The weight factor depends, in general, on B_r^2 and on $\cos\theta$, where θ is the colatitude. As for $(\Delta \tilde{m})_b$, it is the difference in wobble amplitudes between the FOC and the solid region across the boundary b , and $\bar{\eta}_b$ is defined by

$$\begin{aligned} 2\bar{\eta}_b^{1/2} &= \left(\eta_f^{1/2} + \eta_m^{1/2} \right) \\ 2\bar{\eta}_b^{1/2} &= \left(\eta_f^{1/2} + \eta_s^{1/2} \right) \end{aligned} \quad (20)$$

for CMB and ICB, respectively, where η represents magnetic diffusivity and the subscript (f , s , or m) indicates the region (FOC, SIC or mantle layer) to which it pertains:

$$\eta = \left(\sigma^{(el)} \mu_0 \right)^{-1}, \quad (21)$$

$\sigma^{(el)}$ being the electrical conductivity. The term “mantle layer” refers here to a layer at the bottom of the mantle, assumed to have a constant conductivity $\sigma^{(el)}$ throughout and to have a thickness D exceeding the “skin thickness,” i.e., the distance d from the boundary to which the oscillatory induced fields penetrate. It may

be safely said that the conductivity $\sigma_m^{(el)}$ of this layer cannot exceed that of the fluid core and hence that $\eta_m \geq \bar{\eta} \geq \eta_f$. Since d is the reciprocal of the decay constant characterizing the exponential decay of the induced field $\mathbf{b}(\mathbf{r})$ with distance from the CMB within the mantle layer, $d = (2\eta_m/|\omega|)^{1/2}$. The two inequalities $D \geq d$ and $\eta_m \geq \eta_f$ then imply that our assumption of uniform conductivity for the mantle layer requires that

$$D \geq \left(\frac{2\eta_f}{|\omega|} \right)^{1/2}. \quad (22)$$

Since $\mu_0 = 4\pi \times 10^{-7}$, this condition yields $D \geq 209$ m on taking the frequency to be -1 cpsd, the median frequency of the diurnal tidal band, and using the generally accepted value $5 \times 10^5 \text{ S m}^{-1}$ for the conductivity of the core fluid. The conductance of the layer must therefore exceed 10^8 S . If the conductivity of the mantle layer were less than the bound we used or not uniform, the thickness needed for the layer would be higher.

[38] We return now to (19). With the use of parameters appropriate to the relevant boundary, it gives the torque $\tilde{\Gamma}^{\text{CMB}}$ on the FOC due to the magnetic field at the CMB on setting $\Delta \tilde{m} = \tilde{m}_f$ and $\tilde{\Gamma}^{\text{ICB}}$ on the SIC due to the field at the ICB on taking $\Delta \tilde{m} = (\tilde{m}_s - \tilde{m}_f)$. A torque $(-\tilde{\Gamma}^{\text{ICB}})$ is, of course, exerted on the FOC by the SIC. The coupling constants K^{CMB} and K^{ICB} are related to these torques by

$$\begin{aligned} K^{\text{CMB}} &= \frac{\tilde{\Gamma}^{\text{(CMB)}}}{i\Omega_0^2 A_f \tilde{m}_f} \\ K^{\text{ICB}} &= \frac{\tilde{\Gamma}^{\text{(ICB)}}}{i\Omega_0^2 A_s (\tilde{m}_s - \tilde{m}_f)}. \end{aligned} \quad (23)$$

[39] To get an idea of the kind of information that one can get, given an estimate for K^{CMB} , we consider the approximation in which Coriolis effects are neglected. The strength of the coupling between the induction equation and the fluid flow equation is then characterized by a parameter

$$R = \frac{B_r^2}{\mu_0 \rho \bar{\eta} |\omega|}. \quad (24)$$

If the magnetic field is weak enough that $R \ll 1$, the fluid flow remains practically unperturbed by the Lorentz force. In this weak field limit the integral I_b over the CMB reduces to

$$I_b = -2(s+i) \int B_r^2 (1 + \cos^2\theta) ds = -4\pi a_c^2 (s+i) q \langle B_r^2 \rangle, \quad (25)$$

where $s = \sigma/|\sigma|$ and q is a factor which depends on the configuration of the field $\mathbf{B}(\mathbf{r})$. In particular, $q = 16/5$ for a dipole field ($B_r = B_0 \cos\theta$), and $q = 8/3$ for a hypothetical “uniform” field, defined to be one for which B_r is constant over the whole CMB. The latter is not very realistic, but it may be taken as an approximation to a field which is rich in spherical harmonics up to very high orders.

[40] For the forced wobbles, $s = -1$, and we then have from (23) with (19) and (25)

$$\begin{aligned} K^{\text{CMB}} &= (1-i) k^{\text{CMB}} q \left(\frac{\langle B_r^2 \rangle}{\bar{\eta}^{1/2}} \right) \\ k^{\text{CMB}} &= \frac{\pi a_c^4}{\mu_0 \Omega_0 A_f} \left(\frac{1}{2|\omega|} \right)^{1/2}, \end{aligned} \quad (26)$$

with $\bar{\eta}$ given by the first of the expressions in (20). The signs of the real and imaginary parts of (26) are in keeping with the expectations from physical considerations, noted earlier.

[41] Equation (26) shows that the combination $(\langle B_r^2 \rangle / \bar{\eta}^{1/2})$ is known once an estimate is obtained for K^{CMB} . It leads directly to a lower bound on $\langle B_r^2 \rangle$ when the already stated inequality $\bar{\eta} \geq \eta_f$ is introduced in (26):

$$\langle B_r^2 \rangle = \frac{-\text{Im } K^{\text{CMB}}}{q k^{\text{CMB}}} \bar{\eta}^{1/2} \geq \frac{-\text{Im } K^{\text{CMB}}}{q k^{\text{CMB}}} \eta_f^{1/2}. \quad (27)$$

If the thickness D of the mantle layer were less than the skin depth, $\langle B_r^2 \rangle$ would have to be even higher, as may be seen from the work of *Buffett* [1992].

[42] In the weak field approximation on which the above discussion is based, the real and imaginary parts of the coupling constant (K^{CMB} or K^{ICB}) should be of equal magnitude, as (26) shows. Outside the weak field regime, I_b of (19) has to be evaluated by numerical integration. Computations show that with the Coriolis force taken into account, the ratio of the imaginary part of the coupling constant to its real part keeps on decreasing in magnitude as the field strength is increased, and both parts fail to increase as fast as $\langle B_r^2 \rangle$. The reader is referred to *Buffett et al.* [2002] for further details of the treatment and for a discussion of the approximations and assumptions made.

2.5. Inclusion of Ocean Tide Effects

[43] Ocean tides affect nutations through changes in the inertia tensors of the Earth and its core regions due to loading of the crust and through the contribution of ocean tides to the angular momentum of the Earth. The tidal changes in the inertia tensors of the whole Earth and of the fluid core enter into the simplified dynamical equations for an Earth without an inner core [*Sasao and Wahr*, 1981] through

$$\tilde{c}_3 = -A\{\kappa(\tilde{\phi} - \tilde{m}) - \xi \tilde{m}_f\} + \tilde{c}_3^O \quad (28a)$$

$$\tilde{c}_3^f = -A_f\{\gamma(\tilde{\phi} - \tilde{m}) - \beta \tilde{m}_f\} + \tilde{c}_3^{fO}, \quad (28b)$$

where \tilde{c}_3 stands for the complex combination ($c_{13} + ic_{23}$) of elements of the inertia tensor of the whole Earth and \tilde{c}_3^f is the corresponding combination for the fluid core; the superscript O identifies the contributions from ocean loading. According to *Sasao and Wahr* [1981],

$$\tilde{c}_3^O = -A(\tau - \chi)\phi_L, \quad \tilde{c}_3^{fO} = A_f\eta\phi_L, \quad (28c)$$

where ϕ_L is a potential, in dimensionless units, representing the amplitude of the surface load. Parameters τ , χ , and η are those of *Wahr and Sasao* [1981] and are unrelated to the same symbols used elsewhere in this work. Here $\tau = (\Omega_0^2 a^5 / 3GA)$, and $(-\chi/\tau)$ is simply the load Love number k' with the contributions from wobbles turned off. Thus \tilde{c}_3^O is made up of two parts: the direct contribution \tilde{c}_{a3}^O to the inertia tensor from the ocean tide mass and the contribution due to load-induced deformation.

[44] It is clear from the above expressions that ocean loading (OL), in effect, increments the compliances κ and γ by

$$\begin{aligned} \Delta\kappa^{OL} &\equiv -\tilde{c}_3^O / [A(\tilde{\phi} - \tilde{m})] \\ \Delta\gamma^{OL} &\equiv -\tilde{c}_3^{fO} / [A_f(\tilde{\phi} - \tilde{m})], \end{aligned} \quad (29)$$

respectively. When the presence of the inner core is taken into account, one more compliance parameter (θ of *Mathews et al.* [1991a]) gets incremented, but the effect is very small.

[45] Observational estimates for the angular momentum $\tilde{c}_{a3}^O \Omega_0$ are available for the largest few tides such as K_1 , P_1 , O_1 , and Q_1 in the diurnal band [see, e.g., *Chao et al.*, 1996]. On multiplying these by $(\tau - \chi)/(\tau\Omega_0)$, one gets the corresponding \tilde{c}_3^O and hence the $\Delta\kappa^{OL}$ for the respective tides from the first equation in (29). Since $\tilde{c}_3^{fO} = (-A_f/A)[\eta/(\tau - \chi)]\tilde{c}_3^O$ according to (28c), it follows that

$$\Delta\gamma^{OL} = -[\eta/(\tau - \chi)]\Delta\kappa^{OL}. \quad (30)$$

[46] The values thus obtained for $\Delta\gamma^{OL}$ and $\Delta\kappa^{OL}$ exhibit considerable variation from one tide to another. This variation is a reflection of the well-known frequency dependence of the ocean tide admittance that we have referred to earlier. We need a formula expressing this dependence so that the ocean tide contribution to the compliances can be calculated for any desired σ . Our approach to the derivation of such a formula is empirical and makes essential use of a separation of the ocean loading admittance into a product of two factors, following *Wahr and Sasao* [1981]. One factor expresses the frequency dependence due to the FCN resonance; it may be taken to be real for all practical purposes. The second factor, which is complex, represents the effect of other ocean dynamic (OD) factors. Since \tilde{c}_3^O is proportional to the amplitude of the ocean tide height function, $[\tilde{c}_3^O / (\tilde{\phi} - \tilde{m})]$ differs from the admittance function only by a constant factor (it being noted that $\tilde{m}/\tilde{\phi}$ varies only from ~ 0.0032 to 0.0044 over the tidal frequencies that we consider and is practically ignorable in comparison with unity in this context). It will therefore have the same kind of factorized form as the admittance. Thus we take

$$\tilde{c}_3^O / (A\tilde{\phi}) = f_{\text{FCN}} f_{\text{OD}}. \quad (31)$$

[47] Values of f_{FCN} have been given recently by *Desai and Wahr* [1995] for a set of 11 tidal components, updating the values first obtained by *Wahr and Sasao* [1981]. We have found that these can be well fitted by an expression that is linear in $A_e(\sigma)$, the admittance function for a uniform global self-consistent equilibrium ocean:

$$f_{\text{FCN}}(\sigma) = c_0 + c_1 A_e(\sigma). \quad (32)$$

As shown by *Dahlen* [1976],

$$A_e(\sigma) = \frac{1 + k(\sigma) - h(\sigma)}{1 - (3\rho_w/5\rho_E)[1 + k'(\sigma) - h'(\sigma)]}, \quad (33)$$

where k and h are body tide Love numbers for excitation by a degree 2 order 1 potential, k' and h' are the corresponding load Love numbers for the solid Earth, and ρ_w and ρ_E are the density of seawater and the mean density of the Earth, respectively. To determine $A_e(\sigma)$ as a function of frequency, we used the formulae of *Mathews et al.* [1995] expressing the body tide Love numbers as linear combinations of wobble admittances and counterparts of those formulae for the load Love numbers. The coefficients in these combinations were taken from computations by B. A. Buffett (unpublished work, 1995) and the wobble admittances themselves were obtained as functions of σ by solving the dynamical equation (2) for each tidal frequency of interest. The coefficients c_1 and c_2 were then estimated by a least squares fit of (32) to the values of *Desai and Wahr* [1995]. We find that with $c_1 = 0.1732$ and $c_2 = 0.9687$, the fit is good to a fraction of 1%.

[48] The behavior of the factor $f_{\text{OD}}(\sigma)$ representing ocean dynamic effects is expected to be smooth for low spherical

harmonic orders [see, e.g., *Wahr and Sasao*, 1981]. Assuming linear forms

$$f_{OD}^{R,I}(\sigma) = d_0^{R,I} + d_1^{R,I} \sigma \quad (34)$$

for the real (superscript R) and imaginary (superscript I) parts of this factor, we make least squares fits of these to the values found for the real and imaginary parts of $[\tilde{c}_3^O / (A \dot{\phi}_{\text{FCN}})]$ from the ocean mass angular momentum estimates of *Chao et al.* [1996]. The resulting values of the d parameters are $d_0^R = 1.017 \times 10^{-3}$, $d_0^I = -6.287 \times 10^{-4}$, $d_1^R = 8.704 \times 10^{-4}$, and $d_1^I = -4.681 \times 10^{-4}$. On using these as well as the values given above for c_1 and c_2 , we have in (31)–(34) the empirical formula needed for the frequency dependence of $(\tilde{c}_3^O / A \dot{\phi})$. The effective increments to κ and γ due to ocean loading are then obtainable from (29) and (30) for any tidal frequency of interest. One may, for the sake of completeness, determine also the increment to the compliance parameter θ relating to the inner core in a similar way, though its effect on nutations is negligible.

[49] The next concern is about the role of the angular momentum \tilde{h} carried by the ocean tidal current. As shown by *Wahr and Sasao* [1981], this angular momentum enters into the dynamical equation simply through the replacement of \tilde{c}_3^O by $(\tilde{c}_3^O + \tilde{h} / \Omega_0)$. The \tilde{h} term, in effect, adds a further increment $\Delta\kappa^{OC}$ to κ while leaving all other compliances unaffected:

$$\Delta\kappa^{OC} \equiv -(\tilde{h} / \Omega_0) / [A(\dot{\phi} - \tilde{m})]. \quad (35)$$

To derive an empirical formula from which this increment may be evaluated for any tidal constituent, we adopt essentially the same procedure as was described above for ocean loading. The only difference is that we now use the *Chao et al.* [1996] values of \tilde{h} instead of those of $\tilde{c}_3^O \Omega_0$. With this replacement and with the retention of the same f_{FCN} as before one obtains the frequency dependent ocean dynamic factor for tidal currents. We find the d parameters in this case to be $d_0^R = 4.606 \times 10^{-4}$, $d_0^I = 1.049 \times 10^{-4}$, $d_1^R = 4.215 \times 10^{-4}$, and $d_1^I = 2.534 \times 10^{-4}$. One obtains now the overall admittance for ocean tidal currents on multiplying by f_{FCN} the f_{OD} thus determined.

[50] The scope for varying the ocean tide admittance models developed above is limited. We have examined how independent scaling of the load admittance and the current admittance functions by constant factors affects the results of our fit. It was found that the least squares fit is significantly worse if the scale factor for the load admittance function is not very close to unity, but a scale factor of ~ 0.70 is optimal for the current admittance function. Accurate computation of the ocean current angular momentum from ocean tide maps is known to be difficult because of the large contributions to this quantity from small areas where the ocean is very deep. Considering therefore that a scaling of the computed angular momenta by this factor might not be unreasonable, we have incorporated this factor into what we call hereafter the default model for ocean tide effects.

[51] We use the tilde hereafter to identify the (complex) compliances that include the increments due to anelasticity as well as ocean loading and currents effects. For example,

$$\tilde{\kappa} = \kappa + \Delta\kappa, \quad \Delta\kappa \equiv \Delta\kappa^{AE} + \Delta\kappa^{OL} + \Delta\kappa^{OC}, \quad (36)$$

where the superscripts AE , OL , and OC refer to anelasticity, ocean loading, and ocean currents, respectively. Compliances without the tilde will refer strictly to an oceanless elastic Earth. Incorporation of ocean tide and anelastic effects into the theory is accomplished by using the incremented compliances $\tilde{\kappa}$, $\tilde{\gamma}$, etc., in the dynamical equations.

[52] At this point, the dynamical equations including the above effects and electromagnetic couplings are fully determined, given the values assigned to the BEP, provided one knows the ocean tide admittances. This proviso is not trivial. The reason is the interplay of the wobbles, solid Earth tides, and ocean tides (see *Mathews* [2001] for a schematic depiction). The ocean tide admittances for $(nm) = (21)$ are dependent on both the body tide and load Love numbers of the solid Earth, whose dependence on frequency is determined by the wobble admittances of the mantle, the FOC, and the SIC [see, e.g., *Mathews et al.*, 1995] which, in turn, have to be found by solution of the wobble-nutation dynamical equations, the very equations that we are trying to set up. We get over this circularity problem by the use of an iterative process: start with available resonance formulae for the $(nm) = (21)$ Love numbers, from *Wahr and Sasao* [1981], for example, then compute the equilibrium ocean admittance from (33), determine the constants in (32), and then, for both ocean loading and currents, the constants in (34), use the OT load and current admittance functions thus obtained to compute the frequency dependent ocean tide corrections to the compliances in the manner described above, introduce into the dynamical equation the values thus found for the corrections, execute the least squares fitting procedure (to be explained in section 3.3) to estimate the best values for the BEP, solve the dynamical equation with the use of these values to obtain solutions for the wobble admittance functions, and use them to compute the Love number functions. The whole process is iterated until convergence is achieved, making all the functions involved (ocean tide admittances, Love numbers, wobble admittances, etc.) mutually consistent. This iterative process is part of the overall procedure that we have employed.

2.6. Inclusion of Non-TGP Excitations

[53] Atmospheric loading and wind effects on nutations have been discussed in the literature [see, e.g., *Dehant et al.*, 1996; *Bizouard et al.*, 1998; *de Viron et al.*, 1999; *Yseboodt et al.*, 2002]. The atmospheric tides due to the TGP constituents are quite small and are overshadowed by the tides due to heating by the Sun, the largest of these being the solar S_1 thermal tide which affects the prograde annual nutation. Modulation of the amplitude of this tide due to seasonal effects leads one to expect smaller contributions at the prograde semiannual and 121.75 day periods and at the retrograde annual period. There is also a contribution at the K_1 tidal period corresponding to zero frequency in space. Sparseness of atmospheric pressure and wind data (at 12 hour or, at best, 6 hour intervals) and other problems have resulted in wide variations in the theoretical estimates of atmospheric contributions to nutations. *Yseboodt et al.* [2002], analyzing a number of different atmospheric data sets and their subsets, arrive at results as disparate as (18, 114) μs (in phase, out of phase) from one data set and (−65, 10) μs from another for the atmospheric contribution to the prograde annual nutation; the numbers obtained are similarly varied for other nutations too. An additional problem in regard to the prograde annual nutation is that other “Sun-synchronous” effects (having 24 hour periodicity), such as solar heating of VLBI antennas, could affect the observed amplitude. A study of such effects is reported by *Herring et al.* [1991]; it was prompted by the observation of a residual somewhat over 0.1 mas relative to theory (as it was then) in this nutation. A similar residual is found in the present study. In the absence of a reliable means for theoretical estimation of these effects, we have chosen to eliminate the residual by applying the appropriate “correction” to the VLBI estimate for the prograde annual amplitude (in phase and out of phase) before the final fit to theory is done; the role of this nutation in the fit is thus, in effect, nullified.

[54] A contribution to nutations at the annual, semiannual, and 18.6 year periods arises from a general relativistic effect: the geodesic nutation [*Fukushima*, 1991], which accompanies the better known geodesic precession. The geodesic nutation contri-

butions depend only on the parameters of the Earth's orbital motion and are virtually unaffected by the internal dynamics of the Earth. They are therefore the same for the deformable Earth as for the rigid one. Consequently, in using the transfer function to compute the nutation amplitudes for the nonrigid Earth, the geodesic nutation contribution is to be added only to the result obtained by multiplying the relevant rigid Earth amplitude by the value of $T(\sigma; e|e_R)$ corresponding to the frequency involved (and is not to be included in the rigid Earth amplitude).

2.7. Rigid Earth Nutation Amplitudes

[55] In order to use (13) to compute the theoretical values of the nutation amplitudes for fitting to data, one needs to know the rigid Earth nutation amplitudes $\eta_R(\sigma; e_R)$. The computation of the value of $H_d \equiv e/(e+1)$, given the precession rate, is a necessary first step in the construction of rigid Earth nutation series. The rate of “general precession,” which is generally used as the starting point for the evaluation of H_{dR} , is made up of two parts: (1) the “physical” precession (often referred to as the lunisolar precession) consisting of the precessional motion in space of the Earth's principal axis of maximum moment of inertia (not counting the temporally varying tidal deformations) and (2) a contribution due to the motion of the ecliptic in space. It is the rate of the physical precession, which we denote simply by P , that is estimated from VLBI time delay data. It is composed, in turn, of a motion due to relativistic effects, namely, the geodesic precession, and a “classical” (i.e., nonrelativistic) precession due to the gravitational action of celestial bodies on the Earth through H_d and higher moments (J_3, J_4). The equations which govern the classical part of the physical precession and nutation [see, e.g., *Bretagnon et al.*, 1997] have to be solved iteratively, starting with a trial value of H_d , in order to achieve agreement between the observational estimates and the precession rate predicted by these equations, taken together with the geodesic precession. (In reality, the observed precession includes a small contribution due to the nonrigidity of the Earth, a fact which is getting recognized only now.) *Williams* [1994] adopted the value $50287.7 \text{ mas yr}^{-1}$ for the rate of general precession from his assessment of the best available observational data. This value has been the uniform starting point for the computation of H_d in all subsequent works on the nutations of a rigid Earth. Nevertheless, the values obtained for H_d by different authors are unequal: *Bretagnon et al.* [1997] find $H_d = 0.0032737668$, while *Souchay and Kinoshita* [1997] have 0.0032737548 and *Roosbeek and Dehant* [1998] have 0.0032737674 . These are the values employed for H_{dR} in the construction of the respective rigid Earth nutation series. The reasons for the differences among them, small though they are, are not really transparent. The rigid Earth series presented by these authors and a more recent series of *Hartmann et al.* [1999] are all of much higher precision than the earlier series of *Kinoshita and Souchay* [1990] [see also *Souchay and Kinoshita*, 1996, 1997; *Souchay et al.*, 1999; *Bretagnon et al.*, 1998]. Intercomparisons of the different series in the frequency domain are not easy because the sets of fundamental arguments employed by different authors are not identical. However, comparisons in the time domain appear to show close agreement between the different series.

[56] *Williams* [1994] observed for the first time that the 18.6 and 9.3 year terms in the rigid Earth series, having purely lunisolar arguments, nevertheless have out of phase parts due to planetary effects. Inclusion of these parts in our fits do help to reduce the χ^2 . All the recent nutation series show out of phase parts for a number of other terms whose arguments include planetary parts. It may be noted, incidentally, that the geodesic nutation contributions to the nutations in longitude are included in the rigid Earth series of *Roosbeek and Dehant* [1997] but not in *Souchay and Kinoshita* [1999].

[57] All the rigid Earth nutation series present the coefficients of nutation in longitude and obliquity, which have to be transformed

into amplitudes (in general, complex) of the associated circular nutations for use in the context of geophysical theory. A recent formal presentation of the transformation formulae is given by *Defraigne et al.* [1995], though they may also be found in a number of earlier works, e.g., *Herring et al.* [1991] and *Mathews and Shapiro* [1992]. The formulae involve the sine of the mean obliquity, for which we have used the updated value, $\sin \epsilon_0 = 0.3977769687$, adopted by the International Earth Rotation Service for the IERS Conventions 2000.

2.8. Dependence of Nutation Amplitudes on the BEP

[58] In order to identify the BEP other than e that have dominant roles in determining the nutation amplitude $\tilde{\eta}(\sigma)$ it is helpful to examine approximate analytical expressions for the eigenfrequency and resonance strength parameters that appear in the RRF. In doing so, we ignore, for now, the frequency dependence of some of the BEP discussed in section 2.5.

[59] Expressions for the CW, FCN, and PFCN eigenfrequencies, good to $O(\epsilon)$ ($\epsilon \approx 1/300$ being typical of the ellipticities involved in the problem), have been given by *Mathews et al.* [1991a]. Placing tilde symbols over the compliances to indicate inclusion of OT and AE effects, we have

$$\begin{aligned}\sigma_1 &= \frac{A}{A_m}(e - \tilde{\kappa}), \\ \sigma_2 &= -\frac{A}{A_m}(e_f - \tilde{\beta}) - 1, \\ \sigma_3 &= (\alpha_2 e_s + \tilde{\nu}) - 1,\end{aligned}\tag{37}$$

where $(A_s/A_m) \approx 0.0007$ has been neglected in comparison with unity.

[60] We observe now that $(e_f - \tilde{\beta})$ is simply the value of M_{22} of *Mathews et al.* [1991a] for $\sigma = -1$, and $(\alpha_2 e_s + \tilde{\nu})$ is that of $(-M_{33} - M_{34})$. Since the inclusion of electromagnetic couplings is accomplished by the replacements in (18), it becomes evident that the eigenvalues in the presence of CMB and ICB magnetic fields may be obtained by making the replacements

$$\begin{aligned}(e_f - \tilde{\beta}) &\rightarrow (e_f - \tilde{\beta} + K^{\text{CMB}} + K^{\text{ICB}} A_s/A_f) \\ (\alpha_2 e_s + \tilde{\nu}) &\rightarrow (\alpha_2 e_s + \tilde{\nu} - K^{\text{ICB}})\end{aligned}\tag{38}$$

in (37). As for the strengths of the CW and FCN resonances, they are given by

$$\begin{aligned}N_1 &= -\frac{\sigma_1}{e} = -\frac{A}{A_m} \left(1 - \frac{\tilde{\kappa}}{e}\right) \\ N_2 &= \frac{A_f}{A_m} \left(1 - \frac{\tilde{\gamma}}{e}\right)\end{aligned}\tag{39}$$

to $O(\epsilon)$. They remain unaffected by the electromagnetic couplings. The dependence of the PFCN resonance strength N_3 on the BEP is complicated and not particularly revealing. The ICW term in the resonance formula may be ignored because its contribution to $\tilde{\eta}(\sigma)$ is entirely negligible.

[61] It is clear from the considerations of the last two paragraphs that at the stated level of approximation, the locations and strengths of the resonances in the nutation amplitude are determined primarily by e and by a limited number of the BEP appearing through the following combinations:

$$\begin{aligned}p_1 &= (A/A_m)(e - \tilde{\kappa}), \\ p_2 &= (A_f/A_m)(e - \tilde{\gamma}), \\ p_3 &= (A/A_m)(e_f - \tilde{\beta} + K^{\text{CMB}} + K^{\text{ICB}} A_s/A_f), \\ p_4 &= (\alpha_2 e_s + \tilde{\nu} - K^{\text{ICB}}).\end{aligned}\tag{40}$$

Table 1. Nutation Amplitudes and Precession Rate: VLBI Estimates

Period, days	Rigid Earth		VLBI Estimates		Sigma	
	Re	Im	Re	Im	Re	Im
<i>Nutation Amplitudes</i>						
-6798.38	-8050.866	0.078	-8024.825	1.454	0.0095	0.0093
6798.38	-1177.044	0.074	-1180.497	-0.033	0.0095	0.0093
-3399.19	86.742	0.000	86.121	-0.017	0.0045	0.0046
3399.19	3.595	0.003	3.586	0.008	0.0045	0.0046
-1615.75	-0.005	0.000	-0.004	0.020	0.0035	0.0035
1615.75	-0.126	0.000	-0.105	0.005	0.0034	0.0034
-1305.48	0.306	0.000	0.303	0.021	0.0040	0.0040
1305.48	2.099	0.000	2.126	0.020	0.0039	0.0039
-1095.18	0.221	0.000	0.226	0.004	0.0033	0.0033
1095.18	-0.221	0.000	-0.224	0.008	0.0032	0.0032
-386.00	-0.100	0.000	-0.158	0.004	0.0119	0.0007
386.00	-0.689	0.000	-0.709	-0.010	0.0031	0.0031
-365.26	-24.894	0.000	-33.039	0.339	0.0056	0.0067
365.26	25.029	0.000	25.645	0.131	0.0036	0.0036
-346.64	-0.456	0.000	-0.565	-0.003	0.044	0.0040
346.64	-0.067	0.000	-0.063	-0.012	0.0033	0.0034
-182.62	-22.592	0.000	-24.568	-0.059	0.0025	0.0025
182.62	-530.742	0.000	-548.471	-0.499	0.0025	0.0025
-121.75	-0.878	0.000	-0.941	-0.002	0.0025	0.0025
121.75	-20.742	0.000	-21.502	-0.015	0.0025	0.0025
-31.81	-2.882	0.000	-3.059	-0.008	0.0025	0.0025
31.81	3.068	0.000	3.185	0.003	0.0025	0.0025
-27.55	-12.992	0.000	-13.798	-0.050	0.0025	0.0025
27.55	13.964	0.000	14.484	-0.002	0.0025	0.0025
-23.94	0.045	0.000	0.046	-0.007	0.0025	0.0025
23.94	1.144	0.000	1.189	-0.004	0.0025	0.0025
-14.77	-1.121	0.000	-1.200	-0.012	0.0025	0.0025
14.77	1.282	0.000	1.324	-0.003	0.0025	0.0025
-13.78	-0.515	0.000	-0.545	0.000	0.0025	0.0025
13.78	0.595	0.000	0.613	-0.002	0.0025	0.0025
-13.66	-3.404	0.000	-3.639	-0.025	0.0025	0.0025
13.66	-91.517	0.000	-94.196	0.120	0.0025	0.0025
-9.56	-0.084	0.000	-0.085	0.001	0.0025	0.0025
9.56	-2.410	0.000	-2.464	0.014	0.0025	0.0025
-9.13	-0.421	0.000	-0.452	-0.006	0.0029	0.0029
9.13	-12.189	0.000	-12.449	0.035	0.0029	0.0029
-9.12	-0.270	0.000	-0.289	-0.007	0.0029	0.0029
9.12	-2.296	0.000	-2.346	0.011	0.0029	0.0029
-7.10	0.051	0.000	-0.054	-0.002	0.0025	0.0025
7.10	-1.567	0.000	-1.593	0.003	0.0029	0.0029
-6.86	-0.041	0.000	-0.040	-0.001	0.0029	0.0029
6.86	-1.262	0.000	-1.280	-0.002	0.0029	0.0029
<i>Precession Rate Correction (mas/yr)</i>					0.0076	
-2.9601						

These are the parameters to which the nutation amplitudes are most sensitive, apart from the most important of all, namely, e , which occurs as an overall factor in $T(\sigma; e|e_R)$. Clearly, p_1 , p_3 , and p_4 are approximations to σ_1 , $(-\sigma_2 - 1)$, and σ_3 , respectively, and p_2 approximates eN_2 . These along with e are the parameters most suitable for estimation from data.

[62] In setting up the algorithm for least squares fitting, we begin by assigning the values pertaining to Earth model PREM to the moment of inertia ratios that appear in the first three of the p_i . We note that the AE and OT corrections that constitute the differences $(\bar{\kappa} - \kappa)$, $(\bar{\gamma} - \gamma)$, etc., are themselves small and that the errors in the values computed for them in the manner outlined in sections 2.3 and 2.5 are much smaller. It will be presumed therefore that there is no scope for separate adjustment of the OT and AE contributions to κ and γ in the process of making a least squares fit. In particular, the imaginary parts of p_1 and p_2 will not be among the parameters to be estimated through the least squares procedure. (Possible modifications to the anelasticity/ocean tide models, which would affect the contributions to the whole set of compliances, were considered in sections 2.3 and 2.5.) The compliances κ and γ of the basic Earth which appear in Re p_1 and Re

p_2 will, however, be taken for estimation, recognizing that their values could be in error as a consequence of possible errors (for which no estimates are available) in Earth model PREM. In Im p_4 , Im K^{ICB} is the only parameter available for adjustment, and Im p_3 yields another parameter for estimation, namely, Im K^{CMB} . It may be recalled here that the crucial role of Im K^{CMB} in accounting for the out of phase part of the retrograde annual nutation amplitude has been established already by *Buffett* [1992]. Considering next the real part of p_4 , which is the eigenfrequency of the PFCN mode in space, we observe that it involves the combination $[\alpha_2 e_s + \text{Re}(\nu - K^{\text{ICB}})]$. In order to obtain an estimate for Re K^{ICB} , one would need to assume a value for $\alpha_2 e_s$. (The compliance ν is very small, and no significant correction to it is expected.) To begin with, we assign to this quantity the hydrostatic equilibrium value based on PREM. Whether this assignment needs to be changed will have to be considered after examining whether the estimate thus obtained for Re K^{ICB} and the estimate for Im K^{ICB} are mutually compatible in the light of requirements from the theory of the electromagnetic coupling [see *Buffett et al.*, 2002]. The case of Re p_3 , which is the magnitude of the frequency of the FCN in space, is similar. It involves the sum of Re $(K^{\text{CMB}} + K^{\text{ICB}} A_s/A_f)$ and $(e_f - \text{Re } \beta)$. The

fact that estimates from observational data give an excess value for p_3 relative to values computed from typical Earth models has been interpreted in the past purely in terms of an excess value for e_f and hence for the CMB flattening; but part of the excess in p_3 could be attributable to electromagnetic coupling, in which case earlier inferences regarding the excess CMB flattening would be overestimates.

[63] It is of considerable interest to note here that ICB magnetic coupling decreases the eigenfrequency p_3 of the PFCN since $\text{Re } K^{\text{ICB}}$ is positive, as noted earlier. Such a decrease, which would move the eigenperiod from around 475 days [Mathews *et al.*, 1991b] toward longer periods, could cause a noticeable resonant enhancement of the long-period nutations (especially the large 18.6 year nutation), and in this situation, the effect of $\text{Im } K^{\text{ICB}}$ could also be significant. The results of the least squares fit, presented in section 5, show that these expectations are indeed borne out.

[64] It may be appropriate to observe here that the use of astronomical parameters like k_M and k_S [Kinoshita, 1977] as adjustable parameters by Getino and Ferrandiz [1999, 2000a] is in marked contrast to our choice of parameters, though they also employ a number of geophysical parameters including the ratio (A_c/A_m) of the core and mantle moments of inertia, a number of deformability and “dissipation” parameters, and the eigenfrequency of the FCN mode which is really a function of other basic Earth parameters. We shall remark briefly in section 7 on the estimates that they obtain for some of these parameters and their implications.

3. Data and Least Squares Fit

3.1. Data

[65] In this work, the term “input data” or simply “data” will, unless otherwise specified, refer to estimates together with the covariance matrix of the estimates for the first-order lunisolar precession rate and the complex amplitudes of a rather large number of prograde and retrograde nutations. These quantities will be referred to herein as the “observables.” The estimates for the observables are obtained by analysis of a combination of two nutation time series: one from the Goddard Space Flight Center (GSFC) and the other from the U.S. Naval Observatory (USNO), which are derived from raw data sets from largely overlapping series of VLBI experiments. Our input data set is shown in Table 1. The formal standard deviations of the estimated values are shown in the sigma columns. Herring *et al.* [2002] find from intercomparisons of analyses made with distinct data sets and from other tests that the realistic uncertainties should be about twice the formal sigmas for nutation periods under 400 days and considerably higher for periods above 1000 days, probably 4 sigmas for the 18.6 year nutations. Details of the procedures used for and considerations involved in the choice and analysis of VLBI data for generation of our input data may be found in that work.

[66] Note that the rigid Earth nutation series contains several sets of terms having apparently equal periods. However, the arguments of all the terms within any such set are not necessarily the same. Where multiple terms having one of the periods appearing in Table 1 exist in the rigid Earth series, the rigid Earth amplitude shown in Table 1 is the sum of the amplitudes of those members of the multiplet that have identical arguments of lunar-solar origin (i.e., with no planetary component). The observational estimates, of course, include only this subset of terms.

[67] Our estimation process is one of simultaneous least squares fitting of the theoretical expressions for the precession rate P and the nutation amplitude $\tilde{\eta}(\sigma)$ to their observational estimates (the input data set), taking into account the standard deviations and correlations embodied in the variance-covariance matrix forming part of the data set. The quantities to be varied in order to achieve the best fit are the BEP subset identified in section 2.8. What we denote by P here is the “physical” precession rate referred to in

section 2.7. The IAU value of P , from the rate of general precession (50290.966 mas yr⁻¹) based on Lieske *et al.* [1977] and Lieske *et al.*’s value (−96.818 mas yr⁻¹) for the ecliptic motion contribution, is $P_{\text{IAU}} = 50387.784$ mas yr⁻¹. The correction to this value as estimated from VLBI data is part of our input data set, presented in Table 1; it is close to −3 mas yr⁻¹. One obtains the observational estimate P_{obs} on adding this correction to P_{IAU} .

[68] Geodesic nutations, contributions from nonlinear terms present in the full equations of the theory, and contributions from atmospheric tides and other unidentified sources are contained in the observed nutation amplitudes but are not included in our theoretical expressions based on the LDE. The fitting has to be done therefore after removing all such contributions from the input data. The theoretical geodesic nutation contributions are −0.0304, −0.0004, and 0.0001 mas to the prograde annual, semiannual, and 18.6 year nutations, respectively, and 0.0304, 0.0004, and 0.0013 mas to the corresponding retrograde ones. The nonlinear terms contribute −0.0336 and −0.0002 mas to the prograde 18.6 and 9.3 year nutation amplitudes, respectively, and 0.0037 and −0.0022 mas, to the retrograde ones (all in phase). These are subtracted out from the VLBI estimates. (Excluding the sectorial contribution, we find the nonlinear effects on the prograde and retrograde 18.6 year nutations to be −0.0246 and 0.0157 mas respectively, compared to the zonal tide contribution of about −0.038 and 0.028 mas found by Souchay and Folgueira [2000] on the basis of a greatly simplified Earth model.)

[69] Another effect not included in our theory is that of atmospheric variations. From a study of atmospheric pressure and angular momentum data, Bizouard *et al.* [1998] have estimated that the effect on the prograde semiannual nutation should be −20 μ s in phase and 35 out of phase; these numbers are in the middle of the range of values found by Ysebaert *et al.* [2002]. However, our fit with atmospheric effects ignored leaves residuals well under the uncertainties for this nutation: the atmospheric effect has perhaps been cancelled out by some other seasonal effect. In contrast, residuals of somewhat over 100 μ s have been persistently found in the prograde annual nutation. We chose, finally, to interpret the residual found from the present data set in this nutation as the contribution of the S_1 thermal atmospheric tide and other Sun-synchronous effects and removed it (−0.0104 mas in phase and 0.1082 mas out of phase) from the observational data before the final least squares fits, so as to reduce the residual to zero. This contribution and the geodesic nutation and nonlinearity contributions were, of course, added to the postfit theoretical values to arrive at the final nutation series. Theoretical estimates of the atmospheric effect on the retrograde annual nutation from studies using different atmospheric angular momentum data sets varied wildly, and we decided to ignore any contribution to this nutation as well as to the prograde semiannual one.

3.2. Theoretical Representation

[70] The precession rate $P(H_d)$ of the (deformable) Earth with H_d not too far from the value H_{dR} assumed in the rigid Earth theory may be written as

$$P(H_d) = P_R(H_d) + P^{(nr)} = P_R(H_{dR}) + (dP_R/dH_{dR})(H_d - H_{dR}) + P^{(nr)}. \quad (41)$$

The “nonrigidity contribution” $P^{(nr)}$ is due to nonlinear terms in the torque equations, representing the action of spectral components (with $\sigma \neq -1$) of the tesseral tides on the periodic terms in the time-dependent increment to H_d resulting from deformations produced by the zonal and sectorial tides (see Appendix A). Our calculations yielded $P^{(nr)} = -0.2015$ mas yr⁻¹. The residual $\Delta P \equiv P_{\text{obs}} - P(H_d)$, with P_{obs} obtained as in section 3.1, is one of the quantities to be minimized during the least squares fit.

[71] Equation (41) gives the theoretical relation between ΔP and e since $H_d = e/(1 + e)$. In order to make use of this relation in our least squares procedure we need the value of the partial dP_R/dH_{dR} , which is not provided in any of the works on rigid Earth nutation series. This lacuna has been filled through a computation by P. Bretagnon (private communication, 1999), wherein the first-order part of the precession due to H_d alone was isolated and its rate of change with H_d was determined. The value thus found is $dP_R/dH_{dR} = 15397060 \text{ mas yr}^{-1}$.

[72] As for the nutation amplitude, its theoretical representation may be done at one of two levels: either directly in terms of the solution of the dynamical equation or in terms of one of the resonance formulae presented earlier. The latter course offers the attraction of great simplicity of form, but it has to be remembered that the general validity of resonance formulae rests on the assumption of frequency independence of the basic Earth parameters, an assumption which is not really valid because of ocean tide effects, as already noted. For this reason, we chose to obtain the nutation amplitudes $\tilde{\eta}(\sigma)$ by direct solution of the dynamical equations, i.e., by computing $[M^{-1}(\sigma)y(\sigma)]_1$ and then using (13), for each frequency of interest. Default models for anelasticity and ocean tide effects were, of course, incorporated into the dynamical matrix M in the manner described earlier, as were the electromagnetic coupling terms represented simply by the complex free parameters K^{CMB} and K^{ICB} , but not any other effects.

3.3. Fitting of Theory to Data

[73] The observables O_α used in our analysis consist of the correction to the IAU value of the precession rate and the real and imaginary parts of the amplitudes of k pairs of prograde and retrograde nutations. The total number of real observables is thus $N = (4k + 1)$, O_{4k+1} being the precession rate correction and each O_α , $\alpha = 1, \dots, 4k$, being either the real part or the imaginary part of the amplitude $\tilde{\eta}(\sigma)$ of a circular nutation of some particular frequency $\tau = (1 + \sigma)$ cpsd in space. Our input data set (Table 1) has $k = 21$, so that $N = 85$. The full 85×85 covariance matrix is used in the computations. The number n of real parameters P_i to be estimated is 7, as mentioned earlier.

[74] Besides the input data the least squares procedure calls for the matrix B of partials $\partial O_\alpha / \partial P_i$. The P_i chosen for estimation, in the light of the discussion in section 2.8, are e , e_f , κ , γ , $\text{Im } K^{\text{CMB}}$, $\text{Re } K^{\text{ICB}}$ and $\text{Im } K^{\text{ICB}}$. Values based on PREM in hydrostatic equilibrium are adopted for all the other BEP and also for the starting values of e , e_f , κ , and γ . Suitable starting values for the electromagnetic coupling constants are chosen by trial and error. The values of the parameters which are being estimated are updated, of course, at successive stages of the iterative process to be now outlined. At each stage, the matrix $M(\sigma)$ and the vector $y(\sigma)$ in the dynamical equation (2) are evaluated for one frequency σ at a time, and the solution $\tilde{\eta}(\sigma)$ given by (13) is computed. The real and imaginary parts of $\tilde{\eta}(\sigma)$ for a particular σ constitute one pair of O_α . Computation of the partials of this pair is done by making small increments, one at a time, to the values assigned to the various P_i , and reevaluating $\tilde{\eta}(\sigma)$ each time, thereby enabling us to find the rate of change of $\tilde{\eta}(\sigma)$ with respect to each of the P_i . The process is repeated for all the frequencies σ included in the data set. The partials of the precession rate are trivial; the only nonvanishing one, that with respect to e , follows immediately from (41).

[75] Once the matrix B of partials is computed, the corrections to be applied to the initial values of the P_i are obtained through the familiar least squares fitting procedure, and the χ^2 for the fit is evaluated. The initial values are then updated by adding a suitable fraction of these corrections to the earlier values. The whole process is repeated until χ^2 converges to within a predetermined tolerance. The iterative process for the consistent computation of ocean tide contributions, outlined in the penultimate para of section 2.5, then follows.

[76] The updated values of the P_i at the end of the final iteration are the best estimates for these parameters. The standard deviations and mutual correlations of the estimates are also evaluated at this stage. The values of the $\tilde{\eta}(\sigma)$ at the final stage are, for all the σ comprised in the data set, our theoretical values for the nutation amplitudes. Along with these we also have the theoretical value for the precession rate correction, namely, the final value of O_{4k+1} .

4. Least Squares Estimates for the BEP and Residuals of Nutations

[77] We present in Table 2 the values obtained from our fit for the seven estimated parameters (listed in column 1 of the first part of the table) when hydrostatic PREM values are retained for all the other BEP and the default models are employed for anelasticity and ocean tide effects. The adjustment column shows the difference between the values in the estimate column and the corresponding values from hydrostatic equilibrium PREM. The uncertainties shown have been scaled as stated at the end of section 1. The χ^2 per degree of freedom (df) was 7.89, and its square root, 2.80, was the scale factor. The rather high value of χ^2/df is a reflection of the fact that the formal sigmas on the VLBI estimates of the nutation amplitudes underestimate the realistic uncertainties by factors of 2 to 4, as discussed in detail by *Herring et al.* [2002].

[78] It may be noted from the second part of Table 2 that the RMS of the postfit residuals of the 84 (in phase and out of phase) nutation amplitudes is 0.0132 mas compared to 0.0039 for the RMS of the formal sigmas of these amplitudes in the input data set. When it is recalled from section 3.1 that the realistic sigmas are over twice the formal sigmas, it becomes evident that the RMS of postfit residuals differs from the former by less than a factor of 2. In fact, one finds that the RMS of the 64 residuals relating to the nutations with periods under 400 days is just 0.0055 mas, not even twice the RMS of the formal sigmas of the same nutations, which is 0.0033 mas. It is the longer-period nutations which contribute the major share of the RMS of residuals, and this circumstance may be largely a reflection of a large disparity between the formal sigmas of the estimates for such nutations and their realistic uncertainties.

[79] Comparisons have been made between the time series of nutations in longitude and obliquity ($\Delta\psi(t)$ and $\Delta\epsilon(t)$) of the NEOS data set and the time series constructed using the full series of nutation coefficients obtained by direct solution of our dynamical equation. It has been found (D. McCarthy, private communication, 2001) that the weighted RMS of residuals between the two series is 0.182 mas in $\Delta\psi \sin \epsilon$ and 0.184 mas in $\Delta\epsilon$. These are an order of magnitude higher than the RMS of postfit residuals of the major spectral components of nutation used in our analysis. This fact suggests that the VLBI nutation time series contains aliased contributions from inadequacies in modeling of other processes affecting the VLBI, e.g., solid Earth and ocean tides.

4.1. Compliance and Ellipticity Parameters and Precession Rate

[80] It is clear from Table 2 (more specifically, from a comparison of the adjustments with the uncertainties in the estimates column) that the estimates for κ and γ are quite consistent with the values computed from PREM. One can be reasonably confident then that the other compliances (in particular, β and ν , appearing in p_3 and p_4 of (40)) also do not differ significantly from their default values. With the anelasticity and ocean tide contributions to the compliances also treated as fixed and with the term $\alpha_2 e_s$ in p_4 assigned its default value as explained in section 2.8, the least squares process gives us the estimates shown in Table 2 for $\text{Re } K^{\text{ICB}}$ and $\text{Im } K^{\text{ICB}}$. Leaving the discussion of the physical implications of these values to section 4.2, we note that the part of p_3 that still remains unknown is $(e_f + \text{Re } K^{\text{CMB}})$. The second term in this combination needs to be known if we are to obtain an estimate for the ellipticity e_f .

Table 2. Estimates for BEP From Least Squares Fit

BEP	Estimate	Adjustment
e_f	0.0026456 ± 20^a	0.0000973
κ	0.0010340 ± 92	-0.0000043
γ	0.0019662 ± 14	0.0000007
e	0.0032845479 ± 12	0.000037
$\text{Im } K^{\text{CMB}}$	-0.0000185 ± 14	...
$\text{Re } K^{\text{ICB}}$	0.00111 ± 10	...
$\text{Im } K^{\text{ICB}}$	-0.00078 ± 13	...
RMS (sd) _{input}	0.0039	...
RMS residuals	0.0132	...

^aSee text for a discussion of the estimate.

of the fluid core. As we shall see below, it is not possible to come up with a unique estimate for $\text{Re } K^{\text{CMB}}$. However, it appears plausible, for reasons outlined in section 4.2, that its value lies between 1.95×10^{-5} and 2.54×10^{-5} . The estimate shown in Table 2 for e_f corresponds to the choice of the median value of this range for $\text{Re } K^{\text{CMB}}$. If the extreme limits above are considered, the estimates for e_f lie between 0.0026426 and 0.0026485. The excess over the hydrostatic equilibrium value for e_f and, correspondingly, for the CMB flattening is then between 3.7% and 3.9%, instead of $\sim 5\%$ as had been concluded from earlier interpretations of the FCN period inferred from observational data, beginning with *Gwinn et al.* [1986] and *Herring et al.* [1986]. The difference arises, of course, from the fact that the magnetic coupling at the CMB accounts for a part of the deviation of the FCN period from values computed from hydrostatic models with no magnetic couplings.

[81] Our estimate for the dynamic ellipticity e of the whole Earth, shown in Table 2, corresponds to $H_d = 0.0032737949$, which is slightly larger (by ~ 12 ppm) than the H_{dR} employed in the rigid Earth theory of *Souchay and Kinoshita* [1997]. The

uncertainty in the estimate is under four parts in 10^7 . This estimate leads to $P = 50384.788 \pm 0.018$ mas yr^{-1} . Adding to it the updated value -96.865 mas yr^{-1} from *Simon et al.* [1994] for the ecliptic motion contribution, we obtain the estimate 50287.923 ± 0.018 mas yr^{-1} for the rate of general precession. This is slightly higher than the *Williams* [1994] value, namely, 50287.7 mas yr^{-1} .

4.2. Electromagnetic Coupling Constants

[82] The first question that we address is the following: what can we say about the magnetic field at the CMB and about the real part of K^{CMB} , given the estimate of $(-1.85 \pm 0.14) \times 10^{-5}$ found for $\text{Im } K^{\text{CMB}}$? A rough idea about the magnetic field may be obtained from (27) by employing the simple weak field approximation with the neglect of the Coriolis force, considered in section 2.4; one finds that a minimum RMS radial field of somewhere between 4.1 and 4.5 gauss would be needed to account for this coupling if the magnetic field were assumed to be some mix of the uniform and dipole types. The actual field at the CMB is, of course, not that simple. According to estimates by *Langel and Estes* [1982] on the basis of Magsat data, the magnetic field at the CMB has a dipole part with $(B_r)_{\text{RMS}} = 2.64$ gauss; the contributions of higher multipoles have also been estimated by these authors and by *Walker and Backus* [1997]. Pending an investigation of the relation between the RMS field strength and K^{CMB} for magnetic fields with arbitrary spherical harmonic structure, we limit our consideration here to fields which are mixes of the dipole and uniform types. Computations were done for various proportions of the mix, using (23) and (19) together with the general expression given by *Buffett et al.* [2002] for I_b ; all of these were evaluated at the CMB. The curves in Figure 1 show the behavior of $\text{Re } K^{\text{CMB}}$ and $\text{Im } K^{\text{CMB}}$ as functions of the overall $(B_r)_{\text{RMS}}$ for three different mixes of fields of the dipole and uniform types. One of these, in which the ratio of $(B_r)_{\text{RMS}}$ of the dipole part to that of the uniform part is 0.412, is

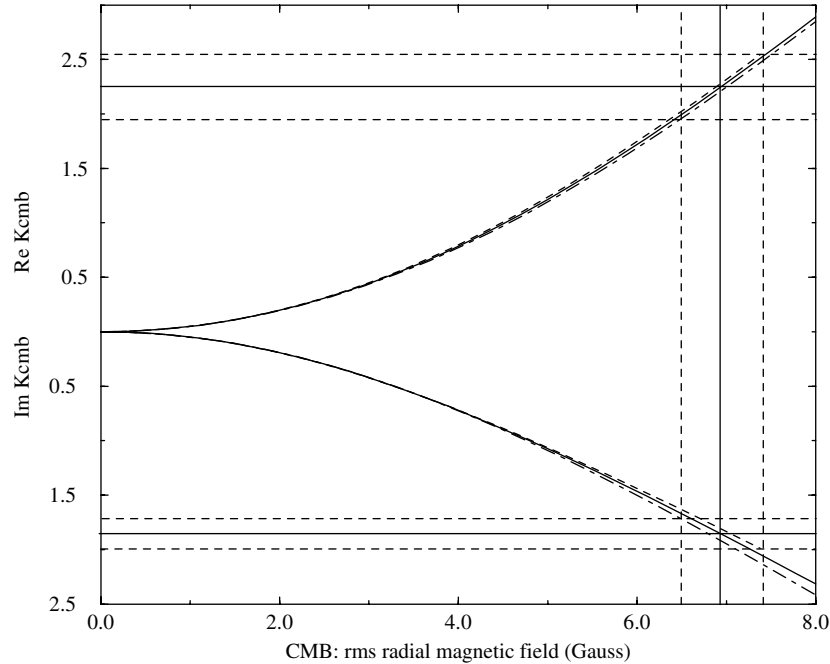


Figure 1. Variation of $\text{Re } K^{\text{CMB}}$ and $\text{Im } K^{\text{CMB}}$ with the RMS radial magnetic field $(B_r)_{\text{RMS}}$ at the CMB for $(B_r)_{\text{RMS}}^{\text{(dipole)}}/(B_r)_{\text{RMS}}^{\text{(uniform)}} = 0.412$ (solid curves), 0.5 (dashed curves), and 0.3 (dash-dotted curves). K^{CMB} is shown in units of 10^{-5} . $\text{Im } K^{\text{CMB}}$ agrees with our estimate of -1.85×10^{-5} in the first case when $(B_r)_{\text{RMS}}^{\text{(dipole)}} = 2.64$ gauss, the *Langel and Estes* [1982] estimate. The solid horizontal line in the lower half of Figure 1 shows the estimate for $\text{Im } K^{\text{CMB}}$ and its intersection with the solid curve yields the estimate of 6.93 gauss for $(B_r)_{\text{RMS}}$ at the CMB; the accompanying dashed lines show the uncertainty limits on $\text{Im } K^{\text{CMB}}$. The intersections of these dashed lines with the curves for $(B_r)_{\text{RMS}}^{\text{(dipole)}}/(B_r)_{\text{RMS}}^{\text{(uniform)}} = 0.5$ and 0.3 provide plausible outer limits on $(B_r)_{\text{RMS}}$ and corresponding limits on $\text{Re } K^{\text{CMB}}$. See text for details.

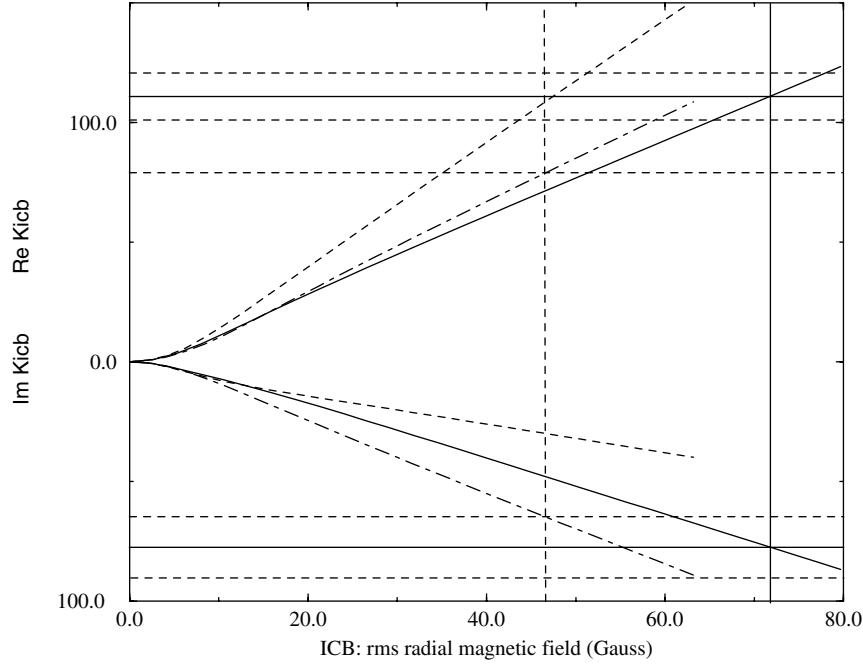


Figure 2. Variation of $\text{Re } K^{\text{ICB}}$ and $\text{Im } K^{\text{ICB}}$ with the RMS radial magnetic field $(B_r)_{\text{RMS}}$ at the ICB for $(B_r)_{\text{RMS}}^{(\text{dipole})}/(B_r)_{\text{RMS}}^{(\text{uniform})} = 0.757$ (solid curves) and for uniform radial fields and pure dipole fields (dash-dotted and dashed curves, respectively). K^{ICB} is shown in units of 10^{-5} . The horizontal solid lines in the upper and lower halves of Figure 2 show the estimated values of $\text{Re } K^{\text{CMB}}$ and $\text{Im } K^{\text{CMB}}$, respectively; the accompanying dashed lines show the uncertainty limits. The estimate for $(B_r)_{\text{RMS}}$ at the ICB is 71.7 gauss, shown by the vertical solid line. The lowest value of $(B_r)_{\text{RMS}}$ consistent with the uncertainty limits on $\text{Im } K^{\text{ICB}}$ is 46 gauss as shown by the dashed vertical line; it calls for a field of the uniform radial type and for a lowered value of 79×10^{-5} for $\text{Re } K^{\text{ICB}}$. See text for discussion.

represented by the solid lines in Figure 1. This mix yields our estimated value for $\text{Im } K^{\text{CMB}}$ when the dipole part has the Langel and Estes value; the corresponding overall $(B_r)_{\text{RMS}}$ is 6.93 gauss. (The estimate for $\text{Im } K^{\text{CMB}}$ is indicated by a horizontal solid line in the lower part of Figure 1, flanked by dashed lines which represent the uncertainty limits on the estimate.) We have shown in Figure 1 two additional cases corresponding to the values 0.3 and 0.5 for the ratio $(B_r)_{\text{RMS}}^{(\text{dipole})}/(B_r)_{\text{RMS}}^{(\text{uniform})}$. Both the real and imaginary branches of the former (dash-dotted curves) lie below the respective solid curves. The dashed curves represent the other case. The overall $(B_r)_{\text{RMS}}$ for which $\text{Im } K^{\text{CMB}}$ agrees with our estimate is ~ 6.79 gauss in the first of these cases and 7.04 gauss in the other. Clearly, the overall field strength needed to account for the observed $\text{Im } K^{\text{CMB}}$ varies little even when the mix of the two types of fields is changed considerably. In view of this insensitivity, we consider it likely that even for more general types of fields containing a dipole part of strength close to the Langel and Estes estimate, the overall $(B_r)_{\text{RMS}}$ needed to generate our value for $\text{Im } K^{\text{CMB}}$ would be somewhere within the bounds set by the curves in Figure 1. When the uncertainty in the estimate of $\text{Im } K^{\text{CMB}}$ is taken into account, these bounds are at 6.5 and 7.4 gauss and are shown by the outer two of the three vertical lines. The intersections of these vertical lines with the real branches of the three curves provide what we consider to be the plausible limits on $\text{Re } K^{\text{CMB}}$: 1.95×10^{-5} and 2.54×10^{-5} .

[83] Turning now to the coupling at the ICB, we show in Figure 2 the variation of the real and imaginary parts of K^{ICB} with $(B_r)_{\text{RMS}}$ at the ICB. The estimates given in Table 2 for these quantities are represented by solid horizontal lines in Figure 2, flanked by dashed lines showing the uncertainty limits on each part. It is assumed, as already mentioned, that the other parameters in p_4 have their default values. In Figure 2, as in Figure 1, the transition from a quadratic dependence of the coupling

constant on the RMS field strength at weak fields to a linear increase for strong fields is evident. It is also evident that the estimate of $(-78 \pm 13) \times 10^{-5}$ for $\text{Im } K^{\text{ICB}}$ and $(111 \pm 10) \times 10^{-5}$ for $\text{Re } K^{\text{ICB}}$ are not mutually compatible for any value of $(B_r)_{\text{RMS}}$ if the field is of either of the pure types (dipole, represented by the dashed curves, or uniform, represented by the dash-dotted curves). However, a mix of the two types with $(B_r)_{\text{RMS}}^{(\text{dipole})}/(B_r)_{\text{RMS}}^{(\text{uniform})} = 0.757$, shown by the solid curves in Figure 2, enables both $\text{Re } K^{\text{ICB}}$ and $\text{Im } K^{\text{ICB}}$ to match our estimates for them. The matching occurs when the RMS values of the radial fields for the uniform and dipole parts are 57.2 and 43.3 gauss, respectively. The overall RMS field is then 71.7 gauss, which is high compared to the field strengths (in the range of 20–35 gauss) that dynamo models appear to lead to. The field strength required could be lowered to ~ 46 gauss (dashed vertical line) by taking a value at the lower end of the uncertainty range for $\text{Im } K^{\text{ICB}}$ and assuming the field to be of the pure uniform type, provided the value needed for $\text{Re } K^{\text{ICB}}$ could be made substantially lower. In order to do this, however, we would have to lower the value of $(\alpha_2 e_s + \nu)$ correspondingly since it is the difference between the two, appearing in the combination p_4 , that influences (and is determined by) nutations. Discussion of the possibilities of accomplishing such a reduction will be deferred to section 7. We go on now to consider a different kind of scenario.

[84] Could it be that the electromagnetic coupling between the FOC and neighboring solid regions is not solely due to the differential wobbles and that we are overestimating the magnetic field strength by attributing the entire electromagnetic torque to this one mechanism? One possibility that might be suggested is that variations in the main field $\mathbf{B}(\mathbf{r})$ caused by dynamo action associated with chaotic convective motion in the fluid core could produce torques comparable to those due to the differential wobbles. In considering this possibility, it is necessary to keep in

Table 3a. Resonance Frequencies, Periods (Uncertainty Limits), and Q^a

Mode	Re σ_α	Im σ_α	Period	Q
1 (CW)	0.002601 ± 10	-0.0001361489 ± 28	(381.9, 385.0)	...
2 (RFCN)	-1.0023181 ± 15	0.0000250 ± 15	(-429.93, -430.48)	20000
3 (PFCN)	-0.99903 ± 10	0.00078 ± 13	(930, 1140)	677
4 (ICW)	0.000413471 ± 42	0.000000319 ± 53	(2411.7, 2412.2)	...

^aAll σ_α values and the CW and ICW periods are in the terrestrial frame; the other two periods are in space. Frequencies are in cpsd, and periods are in mean solar days.

mind (1) that the low-frequency nutations that we are dealing with are caused by the torques due to spectral components of the tesseral tidal potential with frequencies in the retrograde diurnal band in the terrestrial reference frame, (2) that these discrete frequencies lie in a very narrow range between about -0.9 and -1.1 cpsd, and (3) that no spectral frequencies that may be present in the torque other than those present in the line spectrum of these tides are of relevance to the low-frequency nutations. The nature of the high-frequency spectrum of the main field (in the nearly diurnal range) is then the key issue. It seems unlikely that the dynamo mechanism could generate much power at such short periods, although $\mathbf{B}(\mathbf{r})$ does undoubtedly vary on long timescales, perhaps down to periods of several years. In any case, it is to be expected that the spectrum within the very narrow (0.2 cpsd wide) range of interest in the diurnal band is smooth and essentially flat. Consequently, the contributions to the torques at the different tidal frequencies within in this range would be essentially uniform (quite unlike those from the tidally driven differential wobbles which are proportional to the respective tidal amplitudes and so differ from one another by a few orders of magnitude), and their phases would be quite uncorrelated to those of the tidal components. Thus, if the torque between the FOC and the SIC due to the dynamo-generated field is large enough at the frequency σ_{R18} to affect the retrograde 18.6 year nutation to an extent comparable to the contribution ($-101 \mu\text{s}$ in phase and $278 \mu\text{s}$ out of phase) from the differential wobble, its effect at other frequencies would totally swamp the contribution from the differential wobbles. That would have seriously degraded our fit.

[85] To sum up, both theoretical considerations and the evidence from our fit suggest that variations of $\mathbf{B}(\mathbf{r})$ are ignorable in the present context. We do not believe that inaccuracies in our treatment of the electromagnetic torques are responsible for the large estimate for the poloidal field strength at the ICB (or at the CMB), although it is not inconceivable that some relevant physical process has been overlooked in our theory.

5. Resonance Frequencies and Strength Parameters

[86] In constructing an approximate resonance formula in the reduced form (14), we assigned to the ocean tide admittances entering into the dynamical matrix fixed values appropriate to the forcing frequency σ_{R18} which gives rise to the retrograde 18.6 year nutation. The best fit values (from the least squares fit already described) were used for the estimated parameters, while all the other parameters were given the respective default values as before.

The RRF was then constructed using the method outlined in Appendix B after solving the complex eigenvalue equations $M(\sigma)u = 0$ and $\tilde{v}M(\sigma) = 0$, where u and v are four-component columns. (The tilde symbol is used in this particular context to indicate transposition.) The values obtained for the complex frequencies σ_α of the resonances are shown in Table 3a. The corresponding periods are also shown, but the Q factors are listed only for two of the modes, for reasons that will become clear later. The periods shown are, as usual, in the terrestrial frame for the CW and the ICW and in space for the FCN and PFCN. The coefficients N_α of the RRF are given in Table 3b. The RRF may, of course, be recast into an exactly equivalent formula having the unreduced form (8), with the coefficients R_α calculated using the second equation of (15) and R and R' computed then from the sum rules (16). These coefficients are also shown in Table 3b. The numbers in Table 3b do not call for much comment, except for a remainder that N_0 measures the deviation of our estimated value for H_d from the value H_{dR} used in the rigid Earth theory [Souchay and Kinoshita, 1997] that we employed. We proceed therefore to a consideration of the estimates for the eigenfrequencies.

[87] The period of -430.20 ± 0.28 days found for the retrograde free core nutation comes as no surprise, except, perhaps, for the smallness of the uncertainty. The imaginary part of the RFCN resonance frequency, which arises primarily from the dissipative part of the electromagnetic torque, is small enough to lead to a high Q of 20000 for the resonance. However, the effect of this torque, enhanced by the resonance, is large enough to produce a contribution of 0.44 mas to the out of phase amplitude of the retrograde annual nutation and 0.27 mas to that of the retrograde 18.6 year nutation.

[88] The frequency estimate obtained for the PFCN is important in that it provides the first strong observational evidence for the existence of this mode which was predicted on theoretical grounds by Mathews *et al.* [1991a, 1991b] and de Vries and Wahr [1991]. According to our estimate, the real part of the PFCN frequency in space, $\text{Re } \sigma_3 + 1$, is 0.00097 cpsd, which is about half of what was predicted in those works; the uncertainty in the estimate (0.00010 cpsd) is quite small, being $\sim 10\%$. The close proximity of this frequency to those of the 18.6 year nutations causes the effect of the PFCN resonance on the amplitudes of these nutations to be significant. The imaginary part of the PFCN frequency, arising primarily from the dissipative part of the strong ICB electromagnetic coupling, is rather large and results in a relatively low Q of ~ 680 ; $\text{Im } N_3$ is also large, being about one third of the real part in magnitude (see Table 3b). These factors together with the proximity of the PFCN resonance lead to a surprisingly large

Table 3b. Coefficients in the Resonance Formula^a

α	Re N_α	Im N_α	Re R_α	Im R_α
0	1.0000122×10^0	...	4.87871×10^{-2}	1.45661×10^{-3}
P	-2.56699×10^{-1}	-4.28424×10^{-2}
1	-7.91653×10^{-1}	4.14503×10^{-2}	-5.46425×10^{-4}	-7.93218×10^{-5}
2	4.89108×10^{-2}	1.62916×10^{-3}	-1.13686×10^{-4}	-2.55494×10^{-6}
3	2.95844×10^{-4}	-9.57707×10^{-5}	3.62650×10^{-7}	1.37204×10^{-7}
4	-1.50928×10^{-5}	-1.06026×10^{-6}	-4.32089×10^{-8}	-3.03060×10^{-9}

^aRow 0 shows N_0 , and $R_0 = (R - 1)$; row P shows the value of R' .

contribution of 0.28 mas from the ICB electromagnetic coupling to the out of phase part of the retrograde 18.6 year amplitude.

[89] We turn now to the estimate σ_1 given in Table 3a for the Chandler frequency. We shall refer to this estimate as $(\sigma_1)^{R18}$ to call attention to the fact that it was obtained as an eigenvalue of the matrix L with elements evaluated using compliance values pertaining to the excitation frequency corresponding to the retrograde 18.6 year (R18) nutation. This estimate is notable in two respects: the large difference between its real part and the observed Chandler frequency and the negative sign of its imaginary part. The latter feature makes it appear that the free Chandler wobble, given a time dependence $e^{i\sigma_1\Omega_0 t}$, would grow exponentially with time instead of decreasing. The key to the resolution of this apparent paradox lies in the observation that $(\sigma_1)^{R18}$ is not the physical eigenfrequency, i.e., the frequency of the free wobble, but is a resonance frequency: it characterizes the response of the system to excitations in a frequency range (nearly diurnal and retrograde, in the present case) which is far from the frequency of the free mode ($\sim 1/430$ cycles per day and prograde). A resonance frequency is not coincident with the frequency of the free mode, in general, when the system has parameters that are frequency dependent. In the present instance, contributions from both anelasticity and ocean tides to compliance parameters at the observed Chandler frequency are substantially different from those at retrograde diurnal frequencies; see Appendix D for the numerical values of the contributions to κ . The Chandler period is, to a very good approximation, inversely proportional to $(e - \text{Re } \bar{\kappa})$. The differing values of this quantity at σ_{R18} and at low frequencies may therefore be used to calculate the complex eigenfrequency σ_{CW} of the free Chandler period, starting from our estimate $(\sigma_1)^{R18}$ for the resonance frequency to which the seemingly strange period of 383.4 days corresponds. The relation to be used for this purpose is given by (D5). As shown in Appendix D, the free Chandler frequency thus calculated is $(2.3175 + 0.0131i) 10^{-3}$ cpsd. The corresponding period is 430.3 days, which is consistent with observations.

[90] As for the negative sign found for the imaginary part of the estimated Chandler resonance frequency $(\sigma_1)^{R18}$, it is indeed what it should be. This statement is based on general physical considerations, discussed at some length in Appendix C, which lead one to conclude that the imaginary parts of primary response parameters such as compliances must have signs opposite to the sign of the excitation frequency. For the free Chandler wobble, which has a positive frequency, the consequence is that $\text{Im } \sigma_{CW}$ must be positive. This is indeed true of the value shown in the preceding paragraph, which was calculated starting from $\text{Im } (\sigma_1)^{R18}$. The value obtained for Q of the Chandler wobble from the complex σ_{CW} is 88, which is compatible with recent estimates by *Kuehne et al.* [1996] and *Furuya and Chao* [1996], as noted at the end of Appendix D.

[91] The ICW frequency, to the first order, is $(1 - \alpha_2) e_s$, where α_2 is a real parameter independent of any compliances [see *Mathews et al.*, 1991a, equation (30)]. Therefore the imaginary part of σ_{ICW} has to come from second-order terms involving complex compliances and/or the electromagnetic coupling constants. The sign of the imaginary part is determined by the structure of such second-order terms. In the absence of explicit expressions for these terms, there is no obvious way to draw any conclusion as to what the sign should be. There is no incentive to explore this question further, as the ICW resonance term is much too small to make a detectable contribution to nutations.

[92] For the RFCN and PFCN modes the eigenfrequencies lie within the band of excitation frequencies. Consequently, there is no distinction between them and the corresponding resonance frequencies, which unlike σ_1 , do not vary with the forcing frequency: the compliances β and ν on which they depend are not affected by ocean tides and are therefore effectively frequency independent. The imaginary parts of $\sigma_{FCN} \equiv \sigma_2$ and $\sigma_{PFCN} \equiv \sigma_3$ (Table 3a) are both positive, ensuring that the amplitudes of the free modes

decrease with time as they should. The approximate expression for σ_2 given in (37), with the replacement indicated in (38), shows that $\text{Im } \sigma_2 \approx (A/A_m) \text{Im } (\beta - K^{\text{CMB}} - K^{\text{ICB}} A_s/A_f)$. The imaginary part of the compliance β has to be positive for negative frequencies as explained in Appendix C, and $\text{Im } K^{\text{CMB}}$ and $\text{Im } K^{\text{ICB}}$ are both negative (see Table 2). The reason for the positive sign found for $\text{Im } \sigma_2$ is therefore evident. The positive sign of $\text{Im } \sigma_3$ is a consequence of that of the imaginary part of the compliance ν . It is important to note that for the negative frequency (retrograde diurnal) range considered, the signs implied by our $\text{Im } \sigma_\alpha$ for the imaginary parts of all three compliances, κ , β , and ν are identical, which is as it should be.

6. Theoretical Nutation Series

6.1. Series Obtained by Direct Solution of the Dynamical Equation

[93] The new theoretical nutation series for the nonrigid Earth that emerges from our studies is not given by a simple expression like a resonance formula. It is to be constructed by computing the nutation amplitudes in the linearized approximation by the use of (13) and then adding on the contributions from the nonlinear terms in the full dynamical equation and those from non-TGP effects, detailed in section 3.1. The rigid Earth series of *Souchay et al.* [1999] is to be used for $\tilde{\eta}_R(\sigma; e_R)$ in (13), and $M^{-1}(\sigma) y(\sigma)$ is to be evaluated with the use of values from the estimate column of Table 2 for the estimated parameters appearing in M and y and the default values for all other parameters. Anelasticity, ocean tide, and electromagnetic coupling effects are, of course, to be included in the manner described in sections 2.3–2.5. The RMS of residuals between the observations and the new series, which gives an idea of the quality of the overall fit between the two, has already been discussed in the introductory part of section 4.

[94] Table 4 lists our theoretical values for the real and imaginary parts of the amplitudes of a number of nutations. Also shown are the residuals (observed minus theory) and, for comparison, the scaled standard deviations of the corresponding observational estimates. The list includes the 18.6 year, 9.3 year, annual, semi-annual, and fortnightly nutations, which are the most prominent, and all other prograde and retrograde nutations for which the residual in the real or the imaginary part is more than twice the scaled formal standard deviation of the corresponding observational estimate. It may be observed that only two of the 64 in-phase and out of phase residuals pertaining to nutations with periods shorter than 1000 days are in this “large” category, while 57 are within the respective scaled sigmas.

[95] The extent to which anelasticity or other effects influence nutations is of some interest. The individual contributions to some of the prominent nutations are listed in Table 5. As has been already noted, the combined contribution from all the effects does differ in some cases from the total of the individual contributions.

6.2. Nutation Series Expressed in Terms of a New Resonance Formula

[96] The representation of the nutation amplitudes in terms of a resonance formula is obtained by introducing in the first equation of (13) the expression (14) for the generalized transfer function, with parameter values taken from Tables 3a and 3b. The geodesic nutations and other corrections mentioned in section 3.1 are added to the number computed using this representation as well. The theoretical values thus obtained do not fit the observations as well as those of section 6.1. The reason, of course, is the neglect of the frequency dependence of ocean tide admittances, which affects the retrograde annual nutation most of all. The residuals in the real and imaginary parts of this amplitude shoot up to -0.083 and 0.118 mas, respectively. The prograde semiannual nutation is another

Table 4. Theoretical Values From Estimated Parameters and Residuals^a

Period, days	Real Part Nutation Amplitudes, mas			Imaginary Part Nutation Amplitudes, mas		
	Theory	Residual	Uncertainty	Theory	Residual	Uncertainty
−6798.38	−8024.775	−0.050	0.027	1.433	0.022	0.026
6798.38	−1180.459	−0.038	0.027	−0.105	0.072	0.026
−3399.19	86.135	−0.014	0.013	−0.028	0.012	0.013
3399.19	3.614	−0.028	0.013	0.001	0.007	0.013
−1615.75	−0.005	0.001	0.010	0.000	0.020	0.010
1615.75	0.127	0.022	0.010	0.000	0.005	0.010
−365.26	−33.047	0.008	0.016	0.331	0.008	0.019
365.26	25.645	0.000	0.010	0.131	0.000	0.010
−182.62	−24.563	−0.005	0.008	−0.043	−0.016	0.008
182.62	−548.471	−0.000	0.008	−0.502	0.003	0.008
−27.55	−13.807	0.009	0.008	−0.035	−0.015	0.008
−13.66	−3.648	0.009	0.008	−0.013	−0.012	0.008
13.66	−94.198	0.002	0.008	0.124	−0.004	0.008

^aThe estimated correction to P_{IAU} from our fit is -2.997 mas/yr, its residual relative to the observational estimate (with uncertainty of 0.018 mas/yr) is 0.036 mas/yr.

with a considerably increased residual for the imaginary part (0.016 mas) relative to the resonance formula.

[97] Despite such problems the simplicity of a formula of the resonance type for practical use is enticing enough that it was felt necessary to seek a modified formula which gives as close a fit as possible to the exact results of section 6.1. We found that by allowing the parameters N_α and σ_α in (14) to vary linearly with frequency across the diurnal band, the exact results could be reproduced to within $5 \mu\text{s}$ except for the semiannual, retrograde annual, and prograde fortnightly nutations. Formula (14) with such a modification can be recast into the following convenient form, which differs only slightly from (14).

$$T(\sigma; e|e_R) = \frac{e_R - \sigma}{e_R + 1} N_0 \left[1 + (1 + \sigma) \left(Q_0 + \sum_{\alpha=1}^4 \frac{Q_\alpha}{\sigma - s_\alpha} \right) \right]. \quad (42)$$

[98] The procedure for obtaining the new nutation series is then as follows: (1) Take the transfer function $T(\sigma; e|e_R)$ in (13) to be given by (42) with coefficients as in Table 6. (2) Using this transfer function, which is not exact, evaluate the first of the expressions in (13), taking the rigid Earth amplitudes from the series of *Souchay et al.* [1999]. (3) Add the corrections listed in columns 6 and 7 in Table 7 to arrive at the exact values obtainable by direct solution of the LDE. (4) Add the geodesic nutation and other corrections stated in section 3.1 as well as the contributions from the nonlinear terms in the full dynamical equation, all of which are listed in columns 2–5 in Table 7. The end result of this procedure is our new nutation series. All the corrections are shown to 0.0001 mas, although the final precision aimed at for the nutation amplitudes is no more than at the $1 \mu\text{s}$ level. Terms in which the corrections belonging to the last two columns are under $0.5 \mu\text{s}$ are not included in Table 7, excepting a few for which other corrections need to be applied. However, all corrections down to $0.1 \mu\text{s}$ may

be found together with programs for computing the new nutation series at <http://www-gpsg.mit.edu/~tah/mhb2000>. The nonrigidity correction given in the last row of Table 7 is already included in the precession rate estimate given in section 4.1.

7. Discussion and Concluding Remarks

[99] A few remarks may be in order regarding our best fit estimates for e and the corresponding estimate for the precession rate. The amplitudes of all circular nutations depend strongly on the value of e , just as the precession rate does. Consequently, the observed values of each and every nutation amplitude is of relevance to an estimation of e . Our least squares procedure takes advantage of this fact by making use of all the nutation amplitudes estimated from VLBI data together with the precession rate estimate for the estimation of e (along with other BEP). We believe therefore that our result for e is more robust than earlier estimates which have almost always relied solely on the precession rate estimate obtained from VLBI data.

[100] The paper of *Buffett et al.* [2002] sets forth the assumptions and approximations made while deriving the expression which relates the electromagnetic coupling constant to the magnetic field at and the conductivity properties of the media on the two sides of the CMB or the ICB; we do not reproduce them here. In applying their theory to the present work, we have restricted our considerations to special types of magnetic fields. We have assumed, furthermore, that there exists, at the bottom of the mantle, a conducting layer of uniform conductivity equal to that of the core fluid, with thickness D not less than the penetration depth ($\delta \approx 210$ m). Our “best estimate” for $(B_r)_{\text{RMS}}$, with the dipole part required to be 2.64 gauss [*Langel and Estes*, 1982], was 6.9 gauss; it is already somewhat higher than these authors’ estimate of (4.43 ± 2.03) gauss. If the conducting layer were not as thick or were not of uniform conductivity, the magnetic field strength needed to account for

Table 5. Contributions (Re, Im) to Nutations From Individual Effects^a

Period	Anelasticity	OT Load	OT Current	CMB emc	ICB emc
−6798.38	(−0.351, −0.155)	(−0.920, 0.986)	(0.005, −0.020)	(−0.328, 0.249)	(−0.101, 0.278)
6798.38	(0.047, 0.021)	(0.117, −0.126)	(−0.001, 0.003)	(0.037, −0.029)	(0.010, −0.049)
−365.26	(0.267, 0.094)	(0.174, −0.216)	(0.000, −0.001)	(−0.450, 0.411)	(−0.012, 0.017)
365.26	(−0.010, −0.004)	(−0.021, 0.023)	(0.000, −0.001)	(−0.0003, 0.003)	(−0.014, 0.003)
−182.62	(0.034, 0.015)	(0.061, −0.069)	(0.001, −0.002)	(−0.016, 0.012)	(0.000, 0.000)
182.62	(0.287, 0.126)	(0.574, −0.615)	(−0.014, 0.050)	(0.061, −0.047)	(0.026, −0.013)
−13.66	(0.002, 0.001)	(0.006, −0.009)	(0.000, −0.005)	(0.000, 0.000)	(0.000, 0.000)
13.66	(0.095, 0.041)	(0.021, −0.019)	(−0.056, 0.104)	(0.002, −0.001)	(0.000, 0.000)

^aUnits are in mas.

Table 6. Parameters for Use in New Resonance Formula

	Re Part	Im Part
N_0	$1 + 1.224 \times 10^{-5}$...
s_1	3.11279×10^{-3}	3.76098×10^{-4}
s_2	$-1 - 2.31811 \times 10^{-3}$	2.50607×10^{-5}
s_3	$-1 + 9.73555 \times 10^{-4}$	7.78663×10^{-4}
s_4	4.1324×10^{-4}	9.28220×10^{-8}
Q_0	-1.65291×10^{-1}	3.18995×10^{-2}
Q_1	-9.48081×10^{-1}	6.78857×10^{-2}
Q_2	4.89324×10^{-2}	1.61700×10^{-3}
Q_3	2.96114×10^{-4}	-9.56740×10^{-5}
Q_4	-1.10856×10^{-5}	-1.22654×10^{-6}

our estimated value of $\text{Im } K^{\text{CMB}}$ would be even higher. Variations about our best estimate scenario, considered in section 4.2 as proxies for more general field configurations that are yet to be investigated in detail, do not bring the estimated $(B_r)_{\text{RMS}}$ down to within the Langel and Estes range. We are inclined to believe therefore, pending a complete investigation for arbitrary magnetic field configurations, that there is more power in the higher spherical harmonic components of the field at the CMB than has been suggested in interpretations of Magsat data.

[101] Turning now to the ICB, we recall that one cannot estimate $\text{Re } K^{\text{ICB}}$ by itself but only the difference $(\alpha_2 e_s + \nu) - \text{Re } K^{\text{ICB}}$. Therefore, if the actual value of $(\alpha_2 e_s + \nu)$ happens to differ by a certain amount from the default value that we have assumed, the estimate given in Table 2 for $\text{Re } K^{\text{ICB}}$ would stand altered by the same amount. In view of this, we could lower the estimate for $(B_r)_{\text{RMS}}$ from the value given in section 4.2 and thus bring it closer to the range figuring in dynamo theories, if a lower value for $(\alpha_2 e_s + \nu)$ could be justified. Examination of the curves in Figure 2 shows that one could bring the estimate for $(B_r)_{\text{RMS}}$ down to ~ 46 gauss (but no lower) by adopting the lowest magnitude (-64.6×10^{-5}) in the uncertainty range for $\text{Im } K^{\text{ICB}}$ and taking the ICB magnetic field to

be of the purely uniform type, provided that the value of $\text{Re } K^{\text{ICB}}$ could be reduced to the value appropriate for this field, 78.6×10^{-5} . In order to accomplish this, one would have to have $(\alpha_2 e_s + \nu)$ lower than its default value by 32.2×10^{-5} . We examine the possibilities in this regard now.

[102] Consider first the compliance ν . It has been suggested in recent years that the material of the SIC might be in a viscoelastic rather than elastic state. If the deviation from elastic behavior were significant on diurnal timescales, the compliance ν would be complex, and its real part would be larger than the default value of 8×10^{-5} ; the result would be a correspondingly higher estimate for $\text{Re } K^{\text{ICB}}$, which is not what we were seeking. The next candidate is the ellipticity e_s of the SIC. To produce the needed reduction in $(\alpha_2 e_s + \nu)$, e_s would have to be $\sim 16\%$ smaller than in hydrostatic equilibrium, given $\alpha_2 = 0.8294$ [Mathews *et al.*, 1991b]. A mechanism that would produce a decrease of this magnitude in the flattening is hard to find. A third possibility is to have a lower value for α_2 , which is given by the expression

$$\alpha_2 = \frac{A'e'}{A_s e_s} (1 + \alpha_g) - \alpha_g, \quad (43)$$

where α_g is a measure of the strength of the gravitational torque between a tilted inner core and the rest of the Earth [see Mathews *et al.*, 1991a, equation (18)] and A' and e' are the equatorial moment of inertia and dynamical ellipticity, respectively, of a homogeneous ellipsoid of the same dimensions as the SIC but having the same density ρ_f as the core fluid at the ICB. Clearly, A' is proportional to ρ_f and $1 - (A'/A_s)$ is a measure of the fractional density contrast between the inner core and the core fluid at the ICB. Furthermore, α_g is linear in ρ_f . A simple computation shows that a reduction of ρ_f by $\sim 4.6\%$ (i.e., $\sim 560 \text{ kg m}^{-3}$) from its PREM value would lead to a reduction of the magnitude called for above in the value of $(\alpha_2 e_s + \nu)$.

Table 7. Additions and Corrections to (42) and Precession Rate^a

Period, days	Geodesic nutration	Sun-synchronous		Nonlinear Terms	Additional	
		Re	Im		Re	Im
-6798.38	0.0013	0.0037	-0.0002	...
6798.38	0.0001	-0.0336	-0.0007	0.0009
-3339.19	-0.0022	0.0001	-0.0001
3399.19	-0.0002
-439.33	0.0014	0.0012
-416.69	0.0005	0.0002
-411.78	0.0013	-0.0024
-398.88	0.0003	-0.0005
-386.00	-0.0007	0.0009
-365.26	0.0304	-0.0866	0.1072
365.26	-0.0304	-0.0104	0.1082	...	0.0006	-0.0007
-365.23	0.0013	-0.0016
-346.64	-0.0010	0.0012
-182.62	0.0004	-0.0064	0.0073
182.62	-0.0004	-0.0223	0.0231
121.75	-0.0010	0.0010
-31.81	-0.0004	0.0005
-27.55	-0.0020	0.0026
27.55	0.0005	-0.0002
-27.44	-0.0004	0.0005
-13.66	-0.0007	-0.0010
13.66	0.0010	-0.0064
-13.63	-0.0004	0.0006
13.63	0.0002	-0.0012
9.13	0.0008	-0.0019
Precession Rate Correction (mas/yr)						
...	-0.2105

^a The corrections to nutation amplitudes under Geodesic Nutation and Nonlinear Terms columns are to the real Parts of the amplitudes; corrections shown under the Additional column make up for the inexactitude of the resonance formula (42).

[103] To sum up, the estimate from nutation data for the RMS radial field at the ICB is considerably higher than what dynamo theories appear to suggest, and the difference between the estimate and the dynamo regime can be reduced, though not eliminated, by adopting lower values than in hydrostatic equilibrium PREM for the ellipticity of the SIC and/or the density of the core fluid at the ICB. The density ρ_f is of relevance to other phenomena like the translational oscillation modes (Slichter modes) of the SIC, and the Slichter modes will also be influenced by magnetic fields of the order that we are contemplating. Any constraints on ρ_f or relating ρ_f and $\langle B_r^2 \rangle$ that may be obtained in future from such phenomena would help to constrain the ICB magnetic field further.

[104] We expect to complete our treatment of the CMB and ICB electromagnetic couplings through computations of the coupling constants due to magnetic fields of arbitrary spherical harmonic structure. We do not consider it likely that such computations would necessitate any significant changes to the picture that we have presented here.

[105] It may not be out of place to comment here on the fits to nutation data carried out by J. Getino, J. M. Ferrandiz, and collaborators. In the absence of information about fits involving a more complete Earth model, we base our discussion on *Getino and Ferrandiz* [1999]. Two of the critical parameters in their fit were the astronomical parameters k_M and k_S . The value obtained by these authors for ratio k_S/k_M is 0.459194, which is larger than that of *Kinoshita and Souchay* [1990] by one part in 10^4 . But this ratio is essentially a measure of the ratio of the lunar mass to the mass of the Moon-Earth system (the other quantities involved, namely, the mean motions of the Moon and the Sun, being known with much greater precision), and this mass ratio is known to better than one part in 10^9 (see chapter 4 of the IERS Conventions 1996 [*McCarthy*, 1996]). Therefore an adjustment of k_M/k_S to the extent called for by Getino and Ferrandiz seems inadmissible. Again, their estimate of 0.123147 for the ratio A_c/A_m of the moments of inertia of the core and the mantle differs from the PREM value of 0.12758 [see, e.g., *Mathews et al.*, 1991b] by $\sim 3.5\%$; this difference, if interpreted in terms of a change in radius of the CMB, would require a change of over 25 km, as can be readily shown. It is extremely implausible that the seismologically determined CMB radius is open to an adjustment of that order. If the eventual final nutation series by these authors is based on similar parameter fits, the soundness of its astrophysical/geophysical basis would be open to doubt, though it might very well provide an empirical series for practical use if the agreement with observations is good enough.

Appendix A: Nonlinear Terms in the Torque Equation

[106] The torque equation for the whole Earth is

$$\frac{d\mathbf{H}}{dt} + \Omega \times \mathbf{H} = \mathbf{\Gamma}, \quad (\text{A1})$$

where \mathbf{H} is the Earth's angular momentum and $\mathbf{\Gamma}$ is the torque. The equatorial parts of \mathbf{H} and $\mathbf{\Gamma}$ may be represented by

$$\tilde{H} \equiv H_1 + iH_2, \quad \tilde{\Gamma} \equiv \Gamma_1 + i\Gamma_2. \quad (\text{A2})$$

\tilde{h} , H_3 , and $\tilde{\Gamma}$ and hence the torque equation may be separated into parts of different orders in the wobble \tilde{m} , the spin rate perturbation m_3 , and the tidal potential:

$$\begin{aligned} \tilde{H} &= \tilde{H}^{(1)} + \tilde{H}^{(2)}, \\ H_3 &= H_3^{(0)} + H_3^{(1)} + H_3^{(2)}, \\ \tilde{\Gamma} &= \tilde{\Gamma}^{(1)} + \tilde{\Gamma}^{(2)}, \end{aligned} \quad (\text{A3})$$

$$\frac{d\tilde{H}^{(1)}}{dt} + i(\tilde{H}^{(1)} - H_3^{(0)}\tilde{m})\Omega_0 = \tilde{\Gamma}^{(1)} + \tilde{\Delta}^{(2)}, \quad (\text{A4})$$

where all the second-order terms are gathered into $\tilde{\Delta}^{(2)}$:

$$\tilde{\Delta}^{(2)} = \tilde{\Gamma}^{(2)} - \left(\frac{d\tilde{H}^{(2)}}{dt} + i\Omega_0\tilde{H}^{(2)} \right) - i\Omega_0(\tilde{H}^{(1)}m_3 - H_3^{(1)}\tilde{m}). \quad (\text{A5})$$

All the quantities here are taken in the time domain.

[107] Evaluation of the torque may be done directly from its basic definition,

$$\mathbf{\Gamma} = - \int \rho(\mathbf{r})\mathbf{r} \times \nabla \phi(\mathbf{r}; t) dV, \quad (\text{A6})$$

where the integral is over the volume of the Earth and $\rho(\mathbf{r})$ and $\phi(\mathbf{r}; t)$ are the density and the tidal potential, respectively, at the position \mathbf{r} . One obtains the familiar expression $-i(C - A)\dot{\phi}$ for $\tilde{\Gamma}^{(1)}$, where $\tilde{\phi}$ represents the tesseral part of the potential, while $\tilde{\Gamma}^{(2)}$ is found to be given by

$$\tilde{\Gamma}^{(2)} = -i\Omega_0^2 \left[(c_{11}^{(Z)} - c_{33})\tilde{\phi} + (c_{11}^{(S)} - ic_{12})\tilde{\phi}^* \right], \quad (\text{A7})$$

where $c_{11}^{(Z)}$ and $c_{11}^{(S)}$ are the perturbations of the first diagonal element of the Earth's inertia tensor by the zonal and sectorial tidal potentials, respectively. The zonal potential alone is responsible for c_{33} , while c_{12} is due solely to the sectorial part. Note that the spectra of all the terms in (A7) are in the retrograde diurnal band, since the respective spectra of $\tilde{\phi}$ and $\tilde{\phi}^*$ are retrograde and prograde diurnal and the spectra of the zonal and sectorial contributions to the inertia tensor are in the low-frequency and retrograde semidiurnal bands, respectively.

[108] Expressions for the angular momentum quantities herein (of both first and second orders) may be obtained from the defining relations given by *Mathews et al.* [1991a] for \mathbf{H} and for the inertia tensors of the Earth, the FOC, and the SIC. One finds that

$$\tilde{H}^{(1)} = \Omega_0(A\tilde{m} + A_f\tilde{m}_f + A_s\tilde{m}_s + \tilde{c}_3), \quad (\text{A8a})$$

$$H_3^{(0)} = \Omega_0 C, \quad (\text{A8b})$$

$$H_3^{(1)} = \Omega_0(Cm_3 + C_f m_{f3} + C_s m_{s3} + c_{33}), \quad (\text{A8c})$$

where $\Omega_0 m_{f3}$ and $\Omega_0 m_{s3}$ are the axial components of the angular velocities of the FOC and SIC relative to the mantle. The LDE given explicitly by Mathews et al. is the result when one passes over to the frequency domain after introducing such expressions into equation (A4) with the nonlinear part $\tilde{\Delta}^{(2)}$ excluded.

[109] Since $\tilde{\Delta}^{(2)}$ is expected to contribute only a few tens of μs to nutation amplitudes, one can drop the inner core terms and make other simplifications. In particular, the two $\tilde{H}^{(2)}$ terms in $\tilde{\Delta}^{(2)}$, which combine into $(1 + \sigma)\tilde{H}^{(2)}(\sigma)$ in the frequency domain, can be ignored. They yield a negligible contribution because of the factor $(1 + \sigma)$, which is very small for the 18.6 and 9.3 year nutations, and because $\tilde{H}^{(2)}(\sigma)$ itself is too small to be of interest for other frequencies. For similar reasons, the left-hand side of (A4) may be approximated by

$$\frac{d\tilde{H}^{(1)}}{dt} + i(\tilde{H}^{(1)} - H_3^{(0)}\tilde{m})\Omega_0 \rightarrow i\Omega_0^2 A(\sigma - e)\tilde{m} \quad (\text{A9})$$

in the frequency domain for the limited purpose of computing the contribution to \tilde{m} from $\tilde{\Delta}^{(2)}$.

[110] Finally, we observe that on account of the decoupling of the core from the mantle in axial rotation variations, $m_{f3} = -m_3$ and $m_3 = -(c_{33})_m/C_m$ (with the subscript m referring to the mantle). One can then see that

$$\begin{aligned} c_{33} &= -2c_{11}^{(Z)} = -C_{\text{eff}} m_3 \\ C_{\text{eff}} &= C_m / (1 - \gamma C_f / \kappa C), \end{aligned} \quad (\text{A10a})$$

as a consequence of the fact that the radial structure of the deformation of the Earth is the same for zonal, tesseral, and sectorial excitations. The same fact enables us to conclude that

$$c_{11}^{(S)} + ic_{12} = -2\kappa A \tilde{\phi}^{(S)}, \quad (\text{A10b})$$

where the dimensionless sectorial potential $\tilde{\phi}^{(S)}$ is defined in a manner similar to the Mathews *et al.* [1991a] definition of ϕ for the tesseral potential. On using these results in the expression for $\tilde{\Delta}^{(2)}$, we obtain, to an adequate degree of approximation,

$$\begin{aligned} \tilde{\Delta}^{(2)} &= -i\Omega_0^2 \left[(3/2)(C_{\text{eff}} - \kappa A)m_3 \tilde{\phi} - 2\kappa A \tilde{\phi}^{(S)} \tilde{\phi}^* + (C_f + C_{\text{eff}})m_3 \tilde{m} \right. \\ &\quad \left. + A_f m_3 \tilde{m}_f \right]. \end{aligned} \quad (\text{A11})$$

The low-frequency components of m_3 in the products $m_3 \tilde{\phi}$ and $m_3 \tilde{m}$ evidently give rise to retrograde diurnal terms in $\tilde{\Delta}^{(2)}$. One sees also from the spectral expansions

$$\begin{aligned} \tilde{\phi}^{(S)} &= \sum_{\sigma'} \tilde{\phi}^{(S)}(\sigma') e^{i\sigma' \Omega_0 t} \\ \tilde{\phi}^* &= \sum_{\sigma''} \tilde{\phi}^*(\sigma'') e^{-i\sigma'' \Omega_0 t} \end{aligned} \quad (\text{A12})$$

that the frequencies ($\sigma' - \sigma''$) in the product $\tilde{\phi}^{(S)} \tilde{\phi}^*$ are near -1 cpsd since the σ' and σ'' of the sectorial and tesseral tides are close to -2 and -1 cpsd, respectively.

[111] The correction $\delta \tilde{m}(\sigma)$ to $\tilde{m}(\sigma)$ owing to the nonlinear terms may now be obtained by equating to $\tilde{\Delta}^{(2)}(\sigma)$ the corresponding increment to the left-hand side of (A4), which is given, in view of the approximation (A9), by $i\Omega_0^2 A(\sigma - e)\delta \tilde{m}(\sigma)$. For any $\sigma \neq -1$, division of this $\delta \tilde{m}$ by $-(1 + \sigma)$ yields the correction to the corresponding nutation amplitude. The term with $\sigma = -1$ leads to a correction to the precession rate, which may be shown to be $-\Omega_0 \tilde{m}(-1)/\sin \epsilon_0$, where $\epsilon_0 \approx 23.5^\circ$ is the mean obliquity of the Earth's polar axis. Details of the derivations and of justifications for the approximations stated above will be presented elsewhere.

[112] Tables of the axial spin rate variations $\Omega_0 m_3$, denoted by $(\omega - \omega_S)$, are available in the IERS Conventions 1996 [McCarthy, 1996], and those of tesseral and sectorial tides are available in the work by Cartwright and Tayler [1971]. These, taken together with solutions of the LDE, would suffice now for computation of the contributions from the nonlinear terms to nutations.

Appendix B: Evaluation of Parameters in the RRF

[113] Construction of the resonance formula starts with the dynamical matrix M wherein the values of the compliances are made constant by assigning fixed values to the ocean tide admittances as explained in the text. Then M is linear in σ ; so we may write it as

$$M = F\sigma - G, \quad (\text{B1})$$

where F and G are constant matrices with complex elements. The matrix F is nonsingular. The eigenvalues σ_α of our problem, which

are known to be nondegenerate, are to be determined from either of the eigenvalue equations

$$(F\sigma_\alpha - G)u_\alpha = 0, \quad \tilde{v}_\alpha(F\sigma_\alpha - G) = 0, \quad \alpha = 1, \dots, 4, \quad (\text{B2})$$

where \tilde{v}_α are row eigenvectors and u_α are column eigenvectors. Expressing M as

$$M = F(\sigma I - L), \quad L = F^{-1}G, \quad (\text{B3})$$

where I is the unit matrix, we rewrite (B2) in the usual form for eigenvalue equations:

$$\tilde{v}_\alpha L = \sigma_\alpha \tilde{v}_\alpha, \quad Lu_\alpha = \sigma_\alpha u_\alpha. \quad (\text{B4})$$

The matrix L is not symmetric or hermitian, but it does have complete sets of row and column eigenvectors since the eigenvalues are nondegenerate. The two sets are mutually orthogonal and may be so normalized as to make

$$\tilde{v}_\alpha u_\beta = \delta_{\alpha\beta}. \quad (\text{B5})$$

The completeness property then states that

$$\sum_\alpha u_\alpha \tilde{v}_\alpha = I. \quad (\text{B6})$$

[114] Once the solution of the eigenvalue equations, (B4), is carried out, one can express the solution of the forced nutation problem in terms of the eigenvalues and eigenvectors. We start with the spectral expansion

$$(\sigma I - L)^{-1} = \sum_\alpha u_\alpha \frac{1}{\sigma - \sigma_\alpha} \tilde{v}_\alpha. \quad (\text{B7})$$

The problem we seek to solve is $Mx = y$, where the column vector y , being linear in σ , may be written as $y_c + \sigma y_t$. Since $M^{-1} = (\sigma I - L)^{-1}F^{-1}$, we obtain the solution of this inhomogeneous equation with the aid of the spectral expansion (B7) and the completeness relation (B6) as

$$M^{-1}y = F^{-1}y_t + \sum_\alpha \frac{u_\alpha \tilde{v}_\alpha F^{-1}(y_c + \sigma_\alpha y_t)}{\sigma - \sigma_\alpha}. \quad (\text{B8})$$

Each term in (B8) is a four-component column. The first of the elements of the column $M^{-1}y$ is, in view of the dynamical equation (2), the wobble admittance $\tilde{w} \equiv \tilde{m}/\tilde{\phi}$. We thus have the resonance expansion

$$\tilde{w}(\sigma) = w_0 + \sum_\alpha \frac{w_\alpha}{\sigma - \sigma_\alpha} \quad (\text{B9})$$

with

$$w_0 = [F^{-1}y_t]_1, \quad w_\alpha = u_{\alpha 1} [\tilde{v}_\alpha F^{-1}(y_c + \sigma_\alpha y_t)], \quad (\text{B10})$$

where $[F^{-1}y_t]_1$ and $u_{\alpha 1}$ are the first elements of the four-component columns $F^{-1}y_t$ and u_α , respectively. The second element of the column in (B8) yields the resonance expansion for $(\tilde{m}_f/\tilde{\phi})$ and so on.

[115] Now, we know that the value of \tilde{w} at $\sigma = -1$ is the same as for the rigid Earth, namely, $e/(e + 1)$. This property can be used to eliminate w_0 from (B9), leading to the reduced form

$$\tilde{w}(\sigma) = \frac{e}{e+1} + (1+\sigma) \sum_{\alpha} \frac{w_{\alpha}}{1+\sigma_{\alpha}} \frac{1}{\sigma - \sigma_{\alpha}}. \quad (\text{B11})$$

Finally, on dividing by the wobble admittance for the rigid Earth, $\tilde{w}_R(\sigma) = e_R/(e_R - \sigma)$, we obtain the reduced resonance formula for the transfer function given in (12), with

$$N_{\alpha} = \frac{e+1}{e} \frac{w_{\alpha}}{1+\sigma_{\alpha}}. \quad (\text{B12})$$

The expression given in equation (B10) for the w_{α} enables the resonance coefficients N_{α} to be evaluated.

Appendix C: Sign Conventions and Imaginary Parts

C1. Tide-Generating Potential (TGP): Conventions

[116] The convention used in the definition of a constituent of spherical harmonic type (m, n) of the TGP is of special relevance in the representation of the effects of the TGP on a dissipative Earth. In analytic formulations of nutation theory [e.g., *Sasao et al.*, 1980; *Mathews et al.*, 1991a, 1991b], a tidal constituent is expressed as the real part of

$$\phi_{nm}^{(\omega)*}(\mathbf{r}; t) \equiv F_{nm}^{(\omega)}(r) Y_n^m(\theta, \lambda) e^{i\omega t + i\chi(\omega)}, \quad (m \geq 0), \quad (\text{C1})$$

where $F_{nm}^{(\omega)}(r)$ is real and proportional to r^n and the asterisk denotes complex conjugation. In approaches where nutations are treated and computed as part of the complete displacement field produced by the TGP [e.g., *Smith*, 1974; *Wahr*, 1981a, 1981b, 1981c] the convention of *Cartwright and Tayler* [1971] is employed. It differs from that of (C1) in that the space-time dependence is through

$$\phi_{nm}^{(\omega')}(\mathbf{r}; t) \equiv F_{nm}^{(\omega)}(r) Y_n^m(\theta, \lambda) e^{i\omega t + i\chi'(\omega')}. \quad (\text{C2})$$

In either case, the spherical harmonic is defined by

$$Y_n^m(\theta, \lambda) = N_{nm} P_n^m(\cos\theta) e^{im\lambda}, \quad (\text{C3})$$

where P_n^m is the associated Legendre function. Since the real part is to be the same in both cases for a given constituent of the TGP, it is clear that each of the above forms has to be the complex conjugate of the other and hence that

$$\omega' = -\omega, \quad \chi'(\omega') = -\chi(\omega). \quad (\text{C4})$$

The expressions to be used for the nutational and other tidal responses when the TGP is taken in the form (C2) must clearly be complex conjugates of the corresponding expressions that go with (C1).

[117] In the following, we refer to (C1) and (C2) as the $(Y^*, +)$ and $(Y, +)$ representations, respectively, of the TGP. The plus signs here refer to the fact that the time evolution is through $e^{+i\omega t}$ and $e^{+i\omega' t}$. The signs of ω and ω' are determined by the sense of motion of the potential wave. For retrograde motion, the surfaces of constant phase must move westward. With the phase being $(\omega t - m\lambda)$ in the $(Y^*, +)$ representation, it is clear that ω has to be negative for the motion to be retrograde; in the other representation, with the phase being $(\omega' t + m\lambda)$, retrograde motion requires

that ω' be positive. For prograde waves, the signs are reversed. Thus, in the $(Y^*, +)$ representation,

$$\omega < 0, \quad \omega > 0, \quad (\text{C5})$$

for retrograde and prograde, respectively, while in the $(Y, +)$ representation,

$$\omega' > 0, \quad r\omega' < 0, \quad (\text{C6})$$

for retrograde and prograde, respectively.

[118] Tidal waves (except the standing waves for $m = 0$) are all retrograde. There exist, however, a prograde potential wave due to the centrifugal perturbation associated with the Chandler wobble motion which is prograde and others due to the prograde components of ocean tides.

[119] These facts, though elementary, have an important bearing on the representation of the Earth's responses to forcing.

C2. Responses to the Tidal Potential: Conventions

[120] The nutation $\eta(t)$ is the time-dependent offset of the polar axis \mathbf{i}_3 of a suitably defined terrestrial reference system from its mean direction \mathbf{I}_3 which undergoes secular motion because of precession. For an axially symmetric Earth, nutation is due to the periodic components of the $(2, 1)$ part of the TGP. The nutation due to the potential (C1) with $m = 2$, $n = 1$ has the complex representation

$$\tilde{\eta}(t) = i\tilde{\eta}(\sigma) (\mathbf{I}_1 - i\mathbf{I}_2) e^{i\nu\Omega_0 t + i\chi_N(\nu)}, \quad (\text{C7})$$

where \mathbf{I}_1 and \mathbf{I}_2 along with \mathbf{I}_3 constitute a right-handed reference system in space and

$$\nu = 1 + \sigma, \quad \sigma = \omega/\Omega_0. \quad (\text{C8})$$

The tidal Love number parameters, the compliance parameters characterizing the deformabilities of the Earth in response to tidal and centrifugal perturbations, and the nutation amplitude $\tilde{\eta}$ are complex quantities, primarily as a consequence of various dissipative processes: mantle anelasticity, electromagnetic couplings, dissipation in the oceans which affects the ocean tides and their effects on the solid Earth, etc.

[121] A clearly stated convention for the representation of these complex numbers is a matter of importance, as will become evident from the considerations to follow. We adopt the convention that if the $(Y^*, +)$ representation is used for the potential wave, then each of the complex response parameters, say R , will be written as

$$R = R_{\text{in}} + iR_{\text{out}}. \quad (\text{C9})$$

In particular, $\tilde{\eta}$ will be expressed as $\eta_{\text{in}} + i\eta_{\text{out}}$; the Love numbers, for which we use the generic symbol L , will be written as $L_{\text{in}} + iL_{\text{out}}$, etc. It should be self-evident that if we switch to the conjugate representation (C2) for the TGP, the response parameter must be the complex conjugate of (C9); that is, it must be

$$R^* \equiv R_{\text{in}} - iR_{\text{out}}. \quad (\text{C10})$$

Thus the imaginary part of the response parameter changes from R_{out} to $-R_{\text{out}}$ on switching from (C1) to (C2), while R_{out} itself remains unchanged. In particular, the nutation amplitude would switch to $\eta_{\text{in}} - i\eta_{\text{out}}$. For the remainder of Appendix C we adhere to the $(Y^*, +)$ representation.

C3. Responses of Dissipative Earth: Phase Lag

[122] We have used the term “response” above in a very general sense, encompassing both primary and secondary responses. The deformation caused directly by a constituent of the TGP is a primary response; the deformations due to the periodic perturbation of the centrifugal potential caused by the wobbles excited by the TGP are a primary response to the centrifugal perturbation but are a secondary response to the TGP. The compliances appearing in nutation theory are primary deformational response parameters; the Love numbers are not since they include secondary effects due to the wobbles. The wobbles of the mantle and core regions themselves depend in a complicated way on the (primary) compliance parameters and so do the nutations; these are to be classed then as “secondary.” The concept of a phase lag in the response of a dissipative Earth to the driving potential is clearly applicable to primary responses, but the phases of the secondary responses are determined by their functional relationship to the primary response parameters and need not always appear as a lag, especially in the neighborhood of resonances. So the considerations below are restricted to primary responses.

[123] For an excitation of frequency ω , if the response

$$R e^{i\omega t} = |R| e^{i\zeta(\omega)} e^{i\omega t} = |R| e^{i\omega[t + \zeta(\omega)/\omega]} \quad (\text{C11})$$

is to be lagging, it is clearly necessary that

$$\zeta(\omega)/\omega < 0 \quad \text{and hence} \quad \text{Im } R/\omega < 0. \quad (\text{C12})$$

Thus $\text{Im } R$ must have the sign opposite that of the frequency ω . It is of interest to note that *Tromp and Dahlen* [1990] have taken such a link to be self-evident in their analysis of a harmonic oscillator with a complex spring constant, considered as a simple analogy to the anelastic Earth.

[124] Consider the implications of (C12) for the complex compliance $\tilde{\kappa}$. The perturbation of the inertia tensor as well as that of the gravitational potential at the surface of the Earth due to the deformation caused by either the direct action of the tidal potential or by the centrifugal perturbation accompanying the wobble of the whole Earth is directly proportional to κ [see, e.g., *Sasao et al.*, 1980; *Mathews et al.*, 1995]. In the dynamical equations for forced nutation, the tidal forcing frequencies, say ω_T (the subscript T indicating “tidal”), are retrograde ($\omega_T < 0$). The lag condition then requires that the $\tilde{\kappa}$ relevant to forced nutation have

$$\text{Im } \tilde{\kappa}(\omega_T) > 0. \quad (\text{C13})$$

For the potential change or perturbation of the inertia tensor due to the centrifugal deformation accompanying the free Chandler wobble, on the other hand, one must have

$$\text{Im } \tilde{\kappa}(\omega_{CW}) < 0 \quad (\text{C14})$$

since $\omega_{CW} > 0$.

[125] These observations have the interesting consequence, apparently unsuspected hitherto, that the free Chandler wobble, which is an oscillation with a positive frequency, must have a positive sign for the imaginary part of its complex eigenfrequency, while the Chandler resonance frequency determined by the response to forcing at the retrograde diurnal frequencies ω_T must have a negative imaginary part. Both frequencies are given by the same expression,

$$(A/A_m)(e - \tilde{\kappa})\Omega_0,$$

but $\tilde{\kappa}(\omega_{CW})$ has to be used for the compliance in the first case, and $\tilde{\kappa}(\omega_T)$ has to be used in the second. It is a matter for satisfaction that the imaginary part of the Chandler resonance frequency

estimated by us from the fit to VLBI data does have a negative sign, in conformity with the above expectation.

C4. Decay of Free Modes

[126] The property (C14) is demanded also by the requirement that the amplitude of a free wobble of a dissipative Earth be a decreasing function of time. The time evolution of any free wobble being through the factor $e^{i\omega_\alpha t}$, where ω_α is the eigenfrequency of the wobble, a decreasing amplitude for the wobble clearly demands that $\text{Im } \omega_\alpha > 0$. In the case of the Chandler wobble, given the expression $(A/A_m)(e - \tilde{\kappa})\Omega_0$ for ω_{CW} , this requirement translates to $\text{Im } \tilde{\kappa}(\omega_{CW}) < 0$, in agreement with the conclusion (C14) from the lag condition. The same considerations applied to the FCN, taken together with the expression $[-1 - (A/A_m)(e_f - \tilde{\beta})]\Omega_0$ for ω_{FCN} , lead to the requirement that $\text{Im } \tilde{\beta} > 0$, which is in agreement with the demands of the lag condition, $\text{Re } \omega_{FCN}$ being negative.

[127] Finally, it is important to recognize that we arrived at identical signs for the imaginary parts of κ and β for retrograde diurnal (negative) frequencies from different considerations: from the lag condition for the former, and from the decay condition on the free RCFN mode for the latter. It would evidently be strange if different compliances behaved differently at one and the same frequency. It needs to be mentioned in the present context that the signs shown for the imaginary parts of resonance frequencies in a report on an early stage of the efforts to account for the observed nutations [*Mathews and Shapiro*, 1995] are incorrect and should be reversed.

Appendix D: Frequency-Dependent Parameters, Resonance and Eigenfrequencies

[128] We have been concentrating our attention so far on the sign of the imaginary part. We need to consider now other aspects, the importance of which is strikingly illustrated by the consequences of frequency dependence of the magnitudes of the compliances due to anelasticity and ocean tide effects.

[129] Consider the ocean tide produced by a degree 2 tesseral constituent of frequency σ cpsd and amplitude ϕ of the TGP. Nutations are influenced by the deformation due to the loading of the Earth's crust by the $(nm) = (21)$ component, of amplitude t_2 , of the ocean tide. This deformation enters nutation theory through its contributions to \tilde{c}_3 and \tilde{c}_{3f} which represent the off-diagonal components, arising from the direct or indirect action of the TGP, of the inertia tensors of the whole Earth and the FOC, respectively. Ocean loading causes the following replacement of the terms proportional to $(\tilde{\phi} - \tilde{m})$ in the expressions given by *Sasao et al.* [1980] for these quantities:

$$\kappa(\tilde{\phi} - \tilde{m}) \rightarrow \kappa(\tilde{\phi} - \tilde{m}) + \kappa_L \tilde{\phi}_L \quad (\text{D1a})$$

$$\gamma(\tilde{\phi} - \tilde{m}) \rightarrow \gamma(\tilde{\phi} - \tilde{m}) + \gamma_L \tilde{\phi}_L, \quad (\text{D1b})$$

where $\tilde{\phi}_L$ represents the ocean load:

$$\tilde{\phi}_L = \frac{12\pi G \rho_w t_2^1}{5\Omega_0^2 a} \quad (\text{D2})$$

Here ρ_w is the density of seawater, and the loading compliances κ_L and γ_L are the quantities denoted by $\tau - \chi$ and $-\eta$ by *Sasao and Wahr* [1981].

[130] Now we define the dimensionless admittance

$$A(\sigma) = \frac{3}{\Omega_0^2 a^2} \frac{\bar{g} t_2^1}{\tilde{\phi} - \tilde{m}}, \quad (\text{D3})$$

where \bar{g} is the acceleration due to gravity at the mean Earth radius. On substituting (D2) together with (D3) in (D1a) and (D1b) their

right-hand sides become $(\kappa + \Delta\kappa)(\tilde{\phi} - \tilde{m})$ and $(\gamma + \Delta\gamma)(\tilde{\phi} - \tilde{m})$, respectively, where

$$\begin{aligned}\Delta\kappa &= \frac{4\pi G\rho_w a}{5\bar{g}}\kappa_L A(\sigma) \\ \Delta\gamma &= \frac{4\pi G\rho_w a}{5\bar{g}}\gamma_L A(\sigma).\end{aligned}\quad (D4)$$

These are the ocean loading contributions to the compliances. In a treatment which includes the dynamics of the solid inner core [e.g., Mathews *et al.*, 1991a], there is an extra parameter relating to the inner core which gets similarly modified, but its impact is very small.

[131] The ocean response to forcing at low frequencies like σ_{CW} of the Chandler wobble is expected to be of equilibrium nature. The equilibrium admittance is real and is ~ 0.561 according to a computation by C. Bizouard (private communication, 1997). Substitution in (D4) leads to $\Delta\kappa = 1.51 \times 10^{-4}$; it is equivalent to an ocean contribution to the Love number k of ~ 0.044 , which is just about the value obtained by Smith and Dahlen [1981]. A positive $\Delta\kappa$ causes the CW eigenperiod to increase.

[132] Consider now the ocean response to tidal forces in the diurnal band. Ocean tide maps constructed using satellite tracking and altimetry data are available for a few of the prominent diurnal tides (K_1 , P_1 , O_1 and Q_1), and spherical harmonic analyses of these maps yield, among other things, the amplitudes t_2^1 for each of these tides. All these amplitudes lag behind the tidal potential by $\sim 135^\circ$. Using the admittances computed as described in the text, we find that at the frequency -1.0001467 cpsd of the tidal constituent responsible for the retrograde 18.6 year nutation, the increment to κ from ocean loading is $\Delta\kappa^Q = (-5.456 + 5.976i) \times 10^{-5}$ while that due to the ocean current, after scaling by the factor 0.70 employed for optimization of the data fit (see section 2.5), is $\Delta\kappa^C = (-1.448 + 5.515i) \times 10^{-5}$. The total increment to κ from the ocean tide at this frequency is then $\Delta\kappa^T = (-6.904 + 11.491i) \times 10^{-5}$. The negative sign of the real part is important: it causes the period of the Chandler resonance to be lower than for the oceanless Earth.

[133] As for anelasticity, Buffett (unpublished work, 1995) has computed its contributions to the Earth's deformations and hence to the compliances. With the use of the frequency dependence given by (17a) and (17b), one finds that $\Delta\kappa^E$ is $(4.381 - 1.205i) \times 10^{-5}$ for excitation at a period of 430 days, while $\Delta\kappa^E = (1.258 + 0.529i) \times 10^{-5}$ at our retrograde nearly diurnal frequency after scaling of the imaginary part by the factor 1.09 used while fitting the nutation data (see end of section 2.3).

[134] We see from the above numbers that the combined increment from anelasticity and ocean tide effects to κ is $\Delta\kappa(\sigma_{R18}) = (-5.646 + 12.020i) \times 10^{-5}$ at the frequency σ_{R18} , while at the period (≈ 430 days) of the free Chandler wobble it is $\Delta\kappa(\sigma_{CW}) = (19.481 - 1.205i) \times 10^{-5}$. Given these numbers, it becomes possible to infer the frequency σ_{CW} of the free Chandler mode, starting from our estimate for the resonance frequency $(\sigma_1)^{R18}$ given in Table 3a, since

$$\sigma_{CW} = (\sigma_1)^{R18} + (A/A_m)[\Delta\kappa(\sigma_{R18}) - \Delta\kappa(\sigma_{CW})]. \quad (D5)$$

The estimate thus obtained for σ_{CW} is $(2.3175 + .0131i) \times 10^{-3}$, which implies a period of 430.3 days and a Q of 88.4.

[135] It is gratifying that the period thus inferred for the free Chandler wobble is just about what is estimated directly from polar motion data. The value obtained for Q is not unrealistic either, considering the recent estimates by Kuehne *et al.* [1996] ($Q = 72$ or 77 , from two different analyses) and by Furuya and Chao [1996] whose preferred value is 42 but with a one sigma range (33, 100).

[136] **Acknowledgments.** We acknowledge with gratitude the ready help given by many for the investigations presented in this paper, especially

by Dennis McCarthy, Martine Feissel, Ojars Sovers, and Patrick Charlot at various times over the past few years through the supply of estimates obtained by them by analyses of various VLBI data sets for nutation amplitudes and the precession rate, and by Jean Souchay, Fabian Roosbeek and Veronique Dehant, and Pierre Bretagnon, who provided their respective new rigid Earth nutation series prior to publication and kept us updated on improvements. Discussions with some of them and with Jim Williams on various aspects of VLBI data processing, on the one hand, and/or on intricacies of the theory behind the rigid Earth series, on the other hand, have been illuminating. Computations relating to precession, carried out for us by Bretagnon, are gratefully acknowledged, as are also the computations on the equilibrium ocean tide by Christian Bizouard. Special thanks are owed to Hans-Georg Scherneck for elucidating, through extended discussions, various aspects of the modeling of solid Earth deformations due to ocean loading. Information provided by Richard Eanes, Richard Ray, and Olivier deViron about ocean tide modeling and models has been very helpful. One of us (P.M.M.) is particularly indebted and grateful to Irwin Shapiro for constant encouragement and insightful comments and to Veronique Dehant for detailed discussions on a wide variety of subjects touching on this work and for giving generously of her time for reading carefully and making extensive comments and constructive criticisms on successive versions of this paper during its long evolution. He has pleasure in acknowledging the hospitality of Irwin Shapiro and financial support from the Smithsonian Institution which made possible a number of visits at the Harvard-Smithsonian Astrophysical Observatory in Cambridge during the course of this work and the hospitality and support of Veronique Dehant and Paul Paquet for several visits at the Royal Observatory of Belgium in Brussels and to Martine Feissel, Pierre Bretagnon, and Nicole Capitaine for support for visits at the Paris Observatory which provided a multifaceted learning experience. He also wishes to thank David Gubbins for providing the opportunity for a visit with him at the University of Leeds during the nascent stage of this work. Finally, we wish to thank two of the (anonymous) referees for their constructive criticisms and comments, from which we have benefited.

References

- Bizouard, C., A. Brzezinski, and S. Petrov, Diurnal atmospheric forcing and temporal variations of the nutation amplitudes, *J. Geod.*, 72, 561–577, 1998.
- Bretagnon, P., P. Rocher, and J.-L. Simon, Theory of the rotation of the rigid Earth, *Astron. Astrophys.*, 319, 305–317, 1997.
- Bretagnon, P., G. Francou, P. Rocher, and J.-L. Simon, “SMART97”: A new solution for the rotation of the rigid Earth, *Astron. Astrophys.*, 329, 329–338, 1998.
- Bretagnon, P., P. Rocher, and J.-L. Simon, Nonrigid-Earth rotation solution, in *Proceedings of IAU Colloquium 180*, edited by K. J. Johnston *et al.*, pp. 230–235, U.S. Naval Obs., Washington, D. C., 2000.
- Buffett, B. A., Constraints on magnetic energy and mantle conductivity from the forced nutations of the Earth, *J. Geophys. Res.*, 97, 19,581–19,597, 1992.
- Buffett, B. A., P. M. Mathews, T. A. Herring, and I. I. Shapiro, Forced nutations of the Earth: Contributions from the effects of ellipticity and rotation on the elastic deformations, *J. Geophys. Res.*, 98, 21,659–21,676, 1993.
- Buffett, B. A., P. M. Mathews, and T. A. Herring, Modeling of nutation and precession: Effects of electromagnetic coupling, *J. Geophys. Res.*, 10.1029/2000JB000056, 2002.
- Cartwright, D. E., and R. J. Taylor, New computations of the tide-generating potential, *Geophys. J. R. Astron. Soc.*, 23, 45–74, 1971.
- Chao, B. F., R. D. Ray, J. M. Gipson, G. D. Egbert, and C. Ma, Diurnal/semidiurnal polar motion excited by oceanic tidal angular momentum, *J. Geophys. Res.*, 101, 20,151–20,163, 1996.
- Dahlen, F. A., The passive influence of the oceans upon the rotation of the Earth, *Geophys. J. R. Astron. Soc.*, 46, 363–406, 1976.
- de Viron, O., C. Bizouard, D. Salstein, and V. Dehant, Atmospheric torque on the Earth rotation and comparison with the atmospheric angular momentum variations, *J. Geophys. Res.*, 104, 4861–4875, 1999.
- de Vries, D., and J. M. Wahr, The effects of the solid inner core and nonhydrostatic structure on the Earth's forced nutations and Earth tides, *J. Geophys. Res.*, 96, 8275–8293, 1991.
- Defraigne, P., Geophysical model of the Earth dynamical flattening in agreement with the precession constant, *Geophys. J. Int.*, 130, 47–56, 1997.
- Defraigne, P., V. Dehant, and P. Paquet, Link between the retrograde-prograde nutations in obliquity and longitude, *Celestial Mech. Dyn. Astron.*, 62, 363–372, 1995.
- Dehant, V., and P. Defraigne, New transfer functions for nutations of a non-rigid Earth, *J. Geophys. Res.*, 102, 27,659–27,688, 1997.
- Dehant, V., C. Bizouard, J. Hinderer, H. Legros, and M. Leffert, On atmospheric pressure perturbation on precession and nutations, *Phys. Earth Planet. Inter.*, 96, 25–39, 1996.

- Dehant, V., et al., Considerations concerning the non-rigid Earth nutation theory, *Celestial Mech. Dyn. Astron.*, 72, 245–310, 1999.
- Desai, S., and J. M. Wahr, Empirical ocean tide models estimated from TOPEX/Poseidon altimetry, *J. Geophys. Res.*, 100, 25,205–25,228, 1995.
- Dziewonski, A. M., and D. L. Anderson, Preliminary reference Earth model, *Phys. Earth Planet. Inter.*, 25, 297–356, 1981.
- Fukushima, T., Geodesic nutation, *Astron. Astrophys.*, 244, L11–L12, 1991.
- Furuya, M., and B. F. Chao, Estimation of period and Q of the Chandler wobble, *Geophys. J. Int.*, 127, 693–702, 1996.
- Getino, J., and J. M. Ferrandiz, Accurate analytical nutation series, *Mon. Not. R. Astron. Soc.*, 306, L45–L49, 1999.
- Getino, J., and J. M. Ferrandiz, Effects of dissipation and a liquid core on forced nutation in Hamiltonians theory, *Geophys. J. Int.*, 142, 703–715, 2000a.
- Getino, J., and J. M. Ferrandiz, Advances in the unified theory of the rotation of the nonrigid Earth, in *Proceedings of IAU Colloquium 180*, edited by K. J. Johnston et al., pp. 236–241, U.S. Naval Obs., Washington, D. C., 2000b.
- Gilbert, F., and A. M. Dziewonski, An application of normal mode theory to the retrieval of structural parameters and source mechanisms from seismic spectra, *Philos. Trans. R. Soc., Ser. A*, 278, 187–269, 1975.
- Gwinn, C. R., T. A. Herring, and I. I. Shapiro, Geodesy by radiointerferometry: Studies of the forced nutations of the Earth, 2, Interpretation, *J. Geophys. Res.*, 91, 4755–4765, 1986.
- Hartmann, T., M. Soffel, and C. Ron, The geophysical approach towards the nutation of a rigid Earth, *Astron. Astrophys., Suppl. Ser.*, 134, 271–286, 1999.
- Herring, T. A., An apriori model for the reduction of nutation observations: KSV1994.3 nutation series, *Highlights Astron.*, 10, 222–227, 1995.
- Herring, T. A., C. R. Gwinn, and I. I. Shapiro, Geodesy by radiointerferometry: Studies of the forced nutations of the Earth, 1, Data analysis, *J. Geophys. Res.*, 91, 4745–4754, 1986.
- Herring, T. A., B. A. Buffett, P. M. Mathews, and I. I. Shapiro, forced nutations of the Earth: Influence of inner core dynamics, 3, Data analysis, *J. Geophys. Res.*, 96, 8258–8265, 1991.
- Herring, T. A., P. M. Mathews, and B. A. Buffett, Modeling of nutation and precession: Very long baseline interferometry results, *J. Geophys. Res.*, 10.1029/2001JB000165, in Press, 2002.
- Huang, C.-L., W.-J. Jin, and X.-H. Liao, A new nutation model of a non-rigid Earth with ocean and atmosphere, *Geophys. J. Int.*, 145, 1–16, 2001.
- Kinoshita, H., Theory of rotation of the rigid Earth, *Celestial Mech.*, 15, 277–326, 1977.
- Kinoshita, H., and J. Souchay, *Celestial Mech. Dyn. Astron.*, 48, 187–266, 1990.
- Kuehne, J. W., C. R. Wilson, and S. Johnson, Estimates of the Chandler wobble frequency and Q , *J. Geophys. Res.*, 101, 13,573–13,579, 1996.
- Langel, R. A., and R. H. Estes, A geomagnetic field spectrum, *Geophys. Res. Lett.*, 9, 250–253, 1982.
- Lieske, J. H., T. Lederle, W. Fricke, and B. Morando, Expressions for the precession quantities based upon the IAU (1976) System of Astronomical Constants, *Astron. Astrophys.*, 58, 1–16, 1977.
- Mathews, P. M., Consistent modeling of the effects of the diurnal tidal potential, *J. Geodet. Soc. Jpn.*, 47, 219–224, 2001.
- Mathews, P. M., and V. Dehant, Current status of geophysical models of nutation, *Highlights Astron.*, 10, 243–246, 1995.
- Mathews, P. M., and I. I. Shapiro, Nutations of the Earth, *Annu. Rev. Earth Planet. Sci.*, 20, 469–500, 1992.
- Mathews, P. M., and I. I. Shapiro, Recent advances in nutation studies, in *Earth Rotation, Reference Systems in Geodynamics and Solar System, Proceedings of Journees Systemes de Reference Spatio-temporels*, edited by N. Capitaine, B. Kolaczek, and S. Debarbat, pp. 61–66, Space Res. Cent., Warsaw, 1995.
- Mathews, P. M., B. A. Buffett, T. A. Herring, and I. I. Shapiro, Forced nutations of the Earth: Influence of inner core dynamics, 1, Theory, *J. Geophys. Res.*, 96, 8219–8242, 1991a.
- Mathews, P. M., B. A. Buffett, T. A. Herring, and I. I. Shapiro, Forced nutations of the Earth: Influence of inner core dynamics, 2, Numerical results and comparisons, *J. Geophys. Res.*, 96, 8243–8257, 1991b.
- Mathews, P. M., B. A. Buffett, and I. I. Shapiro, Love numbers for diurnal tides: Relation to wobble admittances and resonance expansions, *J. Geophys. Res.*, 100, 9935–9948, 1995.
- McCarthy, D. D., IERS Conventions, *IERS Tech. Note 21*, Int. Earth Rotation Serv., 1996.
- Molodensky, M. S., The theory of nutation and diurnal Earth tides, *Commun. Obs. R. Belg.*, 188, 25–56, 1961.
- Ooe, M., and T. Sasao, Polar wobble, sway and astronomical latitude-longitude observations, *Publ. Int. Latit. Obs. Mizusawa*, 9, 223–233, 1974.
- Poincaré, H., Sur la précession des corps deformables, *Bull. Astron.*, 27, 321–356, 1910.
- Roosbeek, F., and V. Dehant, RDAN97: An analytical development of rigid Earth nutation series using torque approach, *Celestial Mech.*, 70, 215–253, 1998.
- Sailor, R. V., and A. M. Dziewonski, Measurements and interpretation of normal mode attenuation, *Geophys. J. R. Astron. Soc.*, 53, 559–581, 1978.
- Sasao, T., and J. M. Wahr, An excitation mechanism for the free core nutation, *Geophys. J. R. Astron. Soc.*, 64, 729–746, 1981.
- Sasao, T., S. Okubo, and M. Saito, A simple theory on the dynamical effects of a stratified fluid core upon nutational motion of the Earth, in *Proceedings of IAU Symposium 78*, edited by E. P. Federov, M. L. Smith, and P. L. Bender, pp. 165–183, D. Reidel, Hingham, Mass., 1980.
- Schastok, J., A new nutation series for a more realistic model Earth, *Geophys. J. Int.*, 130, 137–150, 1997.
- Seidelmann, P. K., 1980 IAU theory of nutation: The final report of the IAU working group on nutation, *Celestial Mech.*, 27, 79–106, 1982.
- Shirai, T., and T. Fukushima, Numerical convolution in the time domain and its application to the nonrigid-Earth nutation theory, *Astron. J.*, 119, 2475–2480, 2000a.
- Shirai, T., and T. Fukushima, Improvement of nonrigid-Earth nutation theory by adding a model free core nutation term, in *Proceedings of IAU Colloquium 180*, edited by K. J. Johnston et al., pp. 223–229, U.S. Naval Obs., Washington, D. C., 2000b.
- Simon, J.-L., P. Bretagnon, J. Chapront, M. Chapront-Touze, G. Francou, and J. Laskar, *Astron. Astrophys.*, 282, 663–683, 1994.
- Sipkin, S. A., and T. H. Jordan, Frequency dependence of Q_{Scs} , *Bull. Seismol. Soc. Am.*, 70, 1071–1102, 1980.
- Smith, M. L., The scalar equations of infinitesimal elastic-gravitational motion for a rotating, slightly elliptical Earth, *Geophys. J. R. Astron. Soc.*, 37, 491–526, 1974.
- Smith, M. L., and F. A. Dahlen, The period and Q of the Chandler wobble, *Geophys. J. R. Astron. Soc.*, 64, 223–281, 1981.
- Souchay, J., and M. Folgueira, The effect of zonal tides on the dynamical ellipticity of the Earth and its influence on the nutation, *Earth Moon Planets*, 81, 201–216, 2000.
- Souchay, J., and H. Kinoshita, Corrections and new developments in rigid Earth nutation theory, I. Lunisolar influence including indirect planetary effects, *Astron. Astrophys.*, 312, 1017–1030, 1996.
- Souchay, J., and H. Kinoshita, Corrections and new developments in rigid Earth nutation theory, II, Influence of second-order geopotential and direct planetary effect, *Astron. Astrophys.*, 318, 639–652, 1997.
- Souchay, J., B. Loysel, H. Kinoshita, and M. Folgueira, Corrections and new developments in rigid Earth nutation theory, III, Final tables REN-2000 including crossed-nutation and spin-orbit coupling effects, *Astron. Astrophys., Suppl. Ser.*, 135, 111–131, 1999.
- Tromp, J., and F. A. Dahlen, Free oscillations of a spherical anelastic Earth, *Geophys. J. Int.*, 103, 707–723, 1990.
- Wahr, J. M., A normal mode expansion for the forced response of a rotating Earth, *Geophys. J. R. Astron. Soc.*, 64, 651–675, 1981a.
- Wahr, J. M., Body tides on an elliptical, rotating, elastic, and oceanless Earth, *Geophys. J. R. Astron. Soc.*, 64, 677–703, 1981b.
- Wahr, J. M., The forced nutations of an elliptical, rotating, elastic, and oceanless Earth, *Geophys. J. R. Astron. Soc.*, 64, 705–727, 1981c.
- Wahr, J., and Z. Bergen, The effects of mantle anelasticity on nutations, Earth tides, and tidal variations in the rotation rate, *Geophys. J. R. Astron. Soc.*, 87, 633–668, 1986.
- Wahr, J. M., and T. Sasao, A diurnal resonance in the ocean tide and in the Earth's load response due to the resonant free “core nutation”, *Geophys. J. R. Astron. Soc.*, 64, 747–765, 1981.
- Walker, A. D., and G. E. Backus, A six-parameter statistical model of the Earth's geomagnetic field, *Geophys. J. Int.*, 130, 693–700, 1997.
- Widmer, R., G. Masters, and F. Gilbert, Spherically symmetric attenuation within the Earth from normal mode data, *Geophys. J. Int.*, 104, 541–553, 1991.
- Williams, J. G., Contributions to the Earth's obliquity rate, precession and nutation, *Astron. J.*, 108, 711–724, 1994.
- Yseboodt, M., O. de Viron, T. M. Chin, and V. Dehant, Atmospheric excitation of the Earth's nutation: Comparison of different atmospheric models, *J. Geophys. Res.*, 107(B2), 10.1029/2000JB000042, 2002.

B. A. Buffett, Department of Earth and Ocean Sciences, University of British Columbia, 2219 Main Mall, Vancouver, British Columbia, Canada V6T 1Z4. (buffett@geop.ubc.ca)

T. A. Herring, Department of Earth, Atmospheric and Planetary Sciences, Massachusetts Institute of Technology, 77 Massachusetts Avenue, Room 54 618, Cambridge, MA 02138, USA. (tah@mit.edu)

P. M. Mathews, Department of Theoretical Physics, University of Madras (Guindy Campus), Chennai 600025, India. (sonny@eth.net)